Estuarine, Coastal and Shelf Science (2002) **54,** 473–499
doi:10.1006/ecss.2000.0659, available online at http://www.idealibrary.com on IDEAL®

Modelling the Danube-influenced North-western Continental Shelf of the Black Sea. II: Ecosystem Response to Changes in Nutrient Delivery by the Danube River after its Damming in 1972

C. Lancelot[a,e], J. Staneva[b], D. Van Eeckhout[c], J.-M. Beckers[d] and E. Stanev[b]

[a]*Ecologie des Systèmes Aquatiques, Université Libre de Bruxelles, CP 221, Campus Plaine, Bd. du Triomphe, B-1050, Bruxelles, Belgium*
[b]*University of Sofia, Department of Meteorology and Oceanography, 5 James Bourchier Str., BG-1126, Sofia, Bulgaria*
[c]*Bureau Fédéral du Plan, Avenue des Arts, 47–49, B-1000, Bruxelles, Belgium*
[d]*Université de Liège, GHER, Sart-Tilman B5, B-4000, Liège, Belgium*

Received 23 October 1998 and accepted in revised form 17 December 1999

The ecological model BIOGEN, describing the carbon, nitrogen, phosphorus and silicon cycling throughout aggregated chemical and biological compartments of the planktonic and benthic marine systems, has been implemented in the north-western Black Sea to assess the response of this coastal ecosystem to eutrophication by the Danube River. The trophic resolution of BIOGEN was chosen to simulate the major ecological changes reported in this coastal area since the 1960s. Particular attention was paid to establishing the link between quantitative and qualitative changes in nutrients, phytoplankton composition and food-web structures. The BIOGEN numerical code structure includes 34 state variables assembled in five interactive modules describing the dynamics of (1) phytoplankton composed of three distinct groups, each with a different trophic fate (diatoms, nanophytoflagellates, non-silicified opportunistic species); (2) meso- and microzooplankton; (3) trophic dead-end gelatinous organisms composed of three distinct groups (the omnivorous *Noctiluca* and the carnivores *Aurelia* and the alien *Mnemiopsis*), and organic matter degradation and associated nutrient regeneration processes by (4) planktonic and (5) benthic bacteria. The capability of the BIOGEN model to simulate the recent ecosystem changes reported for the Black Sea was demonstrated by running the model for the period 1985–1995. The BIOGEN code was implemented in an aggregated and simplified representation of the north-western Black Sea hydrodynamics. The numerical frame consisted of coupling a 0-D BIOGEN box model subjected to the Danube with a 1-D BIOGEN representing the open-sea boundary conditions. Model results clearly showed that the eutrophication-related problems of the north-western Black Sea were not only driven by the quantity of nutrients discharged by the Danube, but that the balance between them was also important. BIOGEN simulations clearly demonstrated that phosphate, rather than silicate, was the limiting nutrient driving the structure of the phytoplankton community and the planktonic food-web. In particular, it showed that a well-balanced N:P:Si nutrient enrichment, such as that observed in 1991, had a positive effect on the linear, diatom–copepod food-chain, while the regenerated-based microbial food-chain remained at its background level. When present, the gelatinous carnivores also benefited from this enrichment throughout their feeding on copepods. A synergetic effect of fishing pressure and cultural eutrophication was further indirectly suggested by modifying the mortality coefficient of copepods. However, BIOGEN scenarios with unbalanced nutrient inputs, such as nitrogen or phosphate deficiency recorded in 1985 and 1995, predicted the dominance of an active microbial food-web in which bacteria and microzooplankton played a key role; the former as nutrient regenerator, the latter as a trophic path to the copepods and hence to the carnivorous. In such conditions, however, a significant biomass reduction of all gelatinous organisms was simulated, in perfect agreement with recent observations. From these model scenarios it is suggested that the observed positive signs of Black Sea ecosystem recovery might well be related to the reduction of nutrient loads in particular phosphate, by the Danube.

Keywords: eutrophication; ecological modelling; Black Sea; Danube

Introduction

The Black Sea, having unique features, such as being the largest enclosed catchment basin and receiving freshwater and sediment inputs from rivers draining half of Europe and parts of Asia, is very sensitive to the process of eutrophication. In fact, the Black Sea has undergone several changes over the last few decades, driven by human perturbations in the coastal ecosystem itself and in the drainage basins of the rivers. Among these, the Danube River, as the recipient of

[e]Corresponding author. E-mail: lancelot@ulb.ac.be

0272–7714/02/030473+27 $35.00/0

the effluents from eight European countries, affects the north-western Black Sea ecosystem and represents the most significant source of river-borne nutrients flowing into the Black Sea (Tolmazin, 1985). Since the early 1960s, noticeable alterations have been observed at various trophic levels of the Black Sea ecosystem and are well documented. In less than 30 years, the Black Sea has evolved from a highly biologically diverse ecosystem to that of a low biodiversity, dominated by jellyfish (Gomoiu, 1990; Mee, 1992; Bologa *et al.*, 1995). During the late 1980s and early 1990s, there was an almost total collapse of the fisheries industry, which coincided with an unprecedented increase of the jellyfish *Aurelia* and the combjelly *Mnemiopsis,* unintentionally introduced into the Black Sea in the mid-1980s. At that time, it was thought that these unpalatable carnivores—feeding on zooplankton, fish eggs and larvae—were responsible for dramatically reducing the recruitment of fish to the adult carnivore stocks. A comprehensive analysis of existing data (Bologa *et al.*, 1995), in combination with idealized ecological modelling (Van Eeckhout & Lancelot, 1997), however, suggests that the explosive development of jellyfish was the consequence of diverse human activities occurring almost synchronously in the drainage basin of the Danube River and in the marine system. There are: (1) the manipulation of hydrologic regimes of outflowing rivers, in particular the damming in 1972 of the Danube River by the 'Iron Gates', approximately 1000 km upstream (Bondar, 1977); (2) urban and industrial expansion and the intensive use of agricultural fertilizers (Bologa *et al.*, 1984; Gomoiu, 1990; (3) the introduction of exotic species, such as *Mnemiopsis* (Vinogradov & Tumantseva, 1993; Mutlu *et al.*, 1994); and (4) selective and excessive fishing (Ivanov & Beverton, 1985; Stepnowski *et al.*, 1993; Bingel *et al.*, 1993; Gücü, 1997). In particular, increased nutrient loads to the Black Sea modified the quantitative and qualitative nutrient environment of the coastal phytoplankton, increasing nitrogen and phosphorus and lowering silicate (Popa, 1993; Cociasu *et al.*, 1997; Humborg *et al.*, 1997). After 1970, this nutrient change stimulated the development of numerous phytoplankton blooms in summer and led, in general, to the phytoplankton community being dominated by non-siliceous species, some of them of little palatability for mesozooplankton (Bodeanu, 1992; Bologa *et al.*, 1995). As an immediate response to increased primary production, large developments of secondary (copepods) and higher trophic levels (fishes) were first observed (Porumb, 1989). The higher production of fish led to an increase of fish catches and, as a matter of consequence, of fishing pressure (Zaitsev, 1993; Gücü, 1997). By decreasing fish stocks, human activity indirectly stimulated the growth of the gelatinous top predators *Aurelia* and the alien *Mnemiopsis*, which competed for the same food as the fish, but at higher concentrations. This situation accelerated in an explosive way due to the lack of known predators of these gelatinous carnivores and to their voracious feeding on fish eggs and larvae.

Since 1994, however, some positive signs for the recovery of the coastal Black Sea ecosystem have been observed. Phosphorus and nitrogen loads to the Black Sea have considerably decreased, but the Danube concentrations are comparable to other polluted European rivers such as the Rhine, Rhone and Po (Cociasu *et al.*, 1997). Some planktonic and benthic species considered to be extinct or very rare nowadays in the Black Sea have again become common (Lancelot *et al.*, 1998). The abundance of jellyfish has levelled out and the number of anchovy eggs and larvae has increased (Shiganova, 1997). Incidentally, these improvements in the marine ecosystem correspond to the economic decline recorded in Eastern and Central European countries since 1991 (Masaryk & Varley, 1997) (not studied here). The link between human pressures and changes in the marine ecosystem is indeed complex and cannot be understood by simple correlation between historical and ecological events. Mechanistic models, which are based on physical, chemical and biological principles and describe carbon and nutrient cycles as a function of natural and anthropogenic pressures, are ideal tools for handling this complex system. When validated, these mathematical models are of great value in determining the measures to be taken for recovering sustainable water quality and biodiversity in the north-western Black Sea.

As a first step in the direction, the conceptual ecological model BIOGEN (Van Eeckhout & Lancelot, 1997), developed for the analysis of the resistance (or lack of resistance) of the Black Sea ecosystem to destabilization, has been implemented in the Danube-influenced north-western Black Sea. This high trophic-resolution ecological model explicitly describes the bottom-up and top-down controls of the Black Sea pelagic food-chain, and considers the exchanges of nutrients at the water–sediment interface. These properties make it generic and distinct from existing, more simple ecological models developed for the surface layer of the Black Sea (Oguz *et al.*, 1996; Cokasar & Özsoy, 1998; Grégoire *et al.*, 1998). The complexity of the physical features in the Danube-influenced Black Sea continental shelf (Tolmazin, 1985) would ideally require the implementation of BIOGEN in a 3-D frame of high

TABLE 1. Average concentrations of inorganic nutrients at the Danube outflow, calculated for three major periods from Cociasu *et al.*'s (1997) data. Molar ratios are compared with nutrient requirements of coastal diatoms (after Brzezinsky, 1985)

Period	Discharge ($km^3\ yr^{-1}$)	Inorganic nutrients				Molar ratios		
		PO_4 (μM)	SiO (μM)	NO_3 (μM)	NH_4 (μM)	N/P	Si/P	N/Si
1980–1985	210	2·9	69	—	14·8	—	24	
1989–1993	170	4·5	47	232	6·2	54	16	5
1994–1995	191	2·2	36	178	5·8	84	16	5·2
Coastal diatoms						16	16	1

spatio-temporal resolution (Beckers *et al.*, 2000). The complexity of the BIOGEN model makes its direct coupling with the required 3-D physical model scientifically and practically unworkable without a detailed analysis of the ecological features, such as in a more simple frame. As necessary steps before the implementation of the 3-D BIOGEN in the north-western Black Sea, we performed two numerical implementations of the BIOGEN model. Firstly, the BIOGEN model was coupled with a 1-D vertically resolved physical model in order to test the response of the ecological model to changing nutrient conditions in a closed water column. Secondly, the BIOGEN model was implemented as a two-box model resulting from the coupling between the 1-D vertically resolved open-area model and a volume-variable 0-D box model of the coastal area submitted to Danube inputs and bordered at a salinity of 17. This salinity level corresponds to the transition between the Danube-influenced waters and the open Black Sea at a salinity of 18·2 (Ragueneau *et al.*, 2000). The capability of the mathematical tool to simulate the eutrophication-related changes of the Black Sea ecosystem was appraised by running scenarios corresponding to three 'post-Iron Gates' periods with contrasting nutrient loads by the Danube River (Table 1). These are the periods 1980–1985 (nitrogen enriched), 1989–1993 (phosphorus increase and silicic acid impoverishment), and 1995–1997 (decrease of all nutrient concentrations, except for 'nitrate-excess' signature of the out-flowing Danube waters).

BIOGEN model description

General structure

The structure of the BIOGEN model—state variables and processes linking them—is schematically illustrated in Figure 1 and documented in the Appendix (Tables A1 and A2). The model describes the cycling of carbon, nitrogen, phosphorus and silicon through aggregated chemical and biological compartments of the planktonic and benthic systems. Each biological component represents a set of different organisms grouped together according to their trophic level and functional ecological behaviour. BIOGEN thus includes 34 state variables (Appendix, Table A1) assembled in five models. These describe: (1) the growth physiology (photosynthesis, growth, exudation, respiration) of phototrophic flagellates (NF), diatoms (DA) and opportunistic non-siliceous microphytoplankton (OP); (2) the dynamics (grazing, growth, nutrient regeneration, egestion) of the dominant micro- (MCZ) and meso- (COP) zooplankton populations; (3) the feeding and growth activity of the omnivorous giant dinoflagellate *Noctiluca* (NOC) and the carnivorous *Aurelia* (AUR) and *Mnemiopsis* (MNE) gelatinous organisms; (4) the dynamics of organic matter (particulate, POM and dissolved, DOM; each with two classes of biodegradability) degradation by bacteria (BAC) and its coupling with nutrient regeneration; and (5) the benthic diagenesis and nutrient release by local sediments. The model is closed by gelatinous organism mortality and by fish pressure. The latter is indirectly included in the model through the mortality of mesozooplankton (COP) and is described as first-order kinetics.

All forms of major inorganic nutrients are considered. All phytoplankton groups assimilate NO_3, NH_4 and PO_4. Silicic acid (SiO) is taken up only by DA and released into the surrounding medium after diatom lysis and zooplankton feces dissolution. PO_4 and NH_4, the latter only when the chemical composition of the bacterial substrate (BS) is N-depleted, are directly used by bacteria (BAC). Both NH_4 and PO_4 are regenerated through BAC, MCZ, COP, NOC, AUR and MNE catabolic activity. All

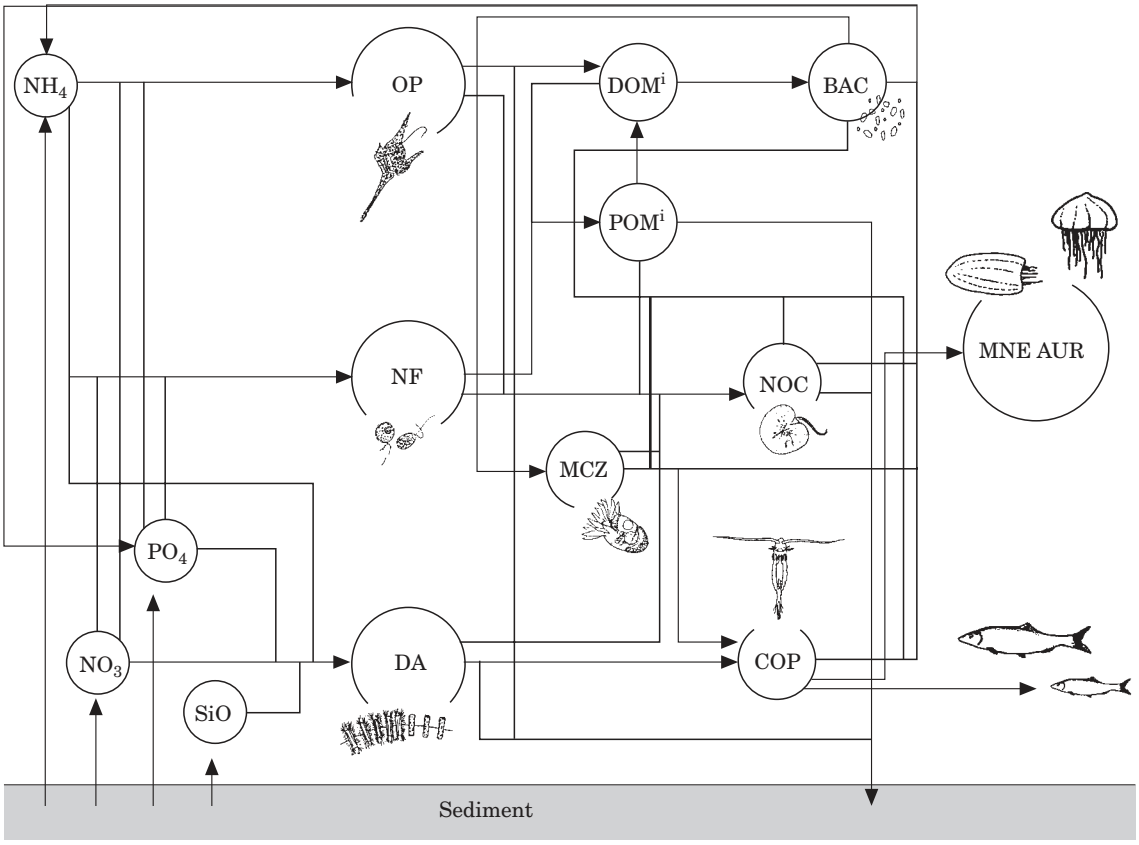

FIGURE 1. Diagrammatic representation of the structure of the BIOGEN model. Inorganic nutrients include ammonium (NH_4), nitrate (NO_3), phosphate (PO_4) and silicic acid (SiO). Organic matter is composed of dissolved ($DOM_{1,2}$) and particulate ($POM_{1,2}$) matter each with two different biodegradability classes. Phytoplankton is composed of three groups: diatoms (DA), autotrophic nanoflagellates (NF) and opportunists (OP). Bacterioplankton is represented by BAC. Zooplankton includes microzooplankton (MCZ) and copepods (COP). The gelatinous food-chain is composed of *Noctiluca* (NOC), *Aurelia* (AUR) and *Mnemiopsis* (MNE).

organisms undergo autolytic processes, which release dissolved (DOM) and particulate (POM) polymeric organic matter, each with two classes of biodegradability, into the water column. Large phytoplankton (DA and OP), detrital particulate organic matter (POM) and zooplankton (COP, NOC, AUR, MNE) fecal pellets undergo sedimentation. Sedimented biogenic material is pooled as benthic particulate organic matter (BPOM) with two classes of biodegradability. Benthic nutrient exchanges are calculated from organic matter degradation, oxygen consumption and nutrient release and transformation (nitrification/denitrification), taking into account PO_4 and NH_4 adsorption on particles and mixing processes in the interstitial and solid phases of the sediment.

Equations and parameterization

The differential equations describing the conservation of state variables are listed in the Appendix (Table A3). The kinetics of processes relative to changes in most biological state variables have been described *in extenso* elsewhere (Billen & Servais, 1989; Billen *et al.*, 1989; Lancelot *et al.*, 1991, 1997*a*, *b*, 2000). Mathematical expressions are listed in the Appendix (Tables A4–A7).

BIOGEN innovation is the representation of the feeding mode of the gelatinous organisms NOC, AUR and MNE. The omnivorous *Noctiluca* (NOC) feed on all auto- and heterotrophic micro-organisms and detrital POM. The gelatinous carnivores AUR and MNE eat mesozooplankton (COP). All gelatinous organisms are ‘ top-predators ’ and no trophic link exists between them. Thus, lysis is the only mortality process affecting them. The feeding mechanisms of the gelatinous organisms have been shown to greatly differ from that of copepods and microzooplankton. The latter are described by Monod-type kinetics with saturation of the specific ingestion rate at high food concentrations (Appendix, Table A5).

Conversely, observations (Hoffmeyer, 1990) show that, above a minimum food threshold, the specific food ingestion rate of gelatinous organisms (omnivorous and carnivorous) increases linearly with respect to food without saturation at high concentration. The corresponding mathematical expression is given in the Appendix (Table A5).

The parameterization procedure constitutes a key step for the successful implementation of a mechanistic model and the assessment of its prediction capability. Most biological parameters were derived from process-level measurements conducted during the 1995 and 1997 EROS cruises of the RV *Professor Vodyanitsky*, as well as from other relevant literature data. Additionally, a large number of numerical process-oriented sensitivity studies have been carried out to understand the model's response in different conditions. The sensitivity experiments were directed towards (1) tuning the set of unknown or poorly defined biological parameters and (2) investigating the response of the ecosystem to the initial conditions. All sensitivity analyses were carried out with the 0-D version of the BIOGEN model (Staneva, unpubl. data) and will be described elsewhere. BIOGEN parameters are summarized in the Appendix (Table A4–A7).

Model implementations

1-D BIOGEN

The BIOGEN model was coupled with the vertically resolved 1-D physical model of Staneva *et al.* (1998). This model is a 1-D-turbulent hydrodynamical model that calculates the thickness of the wind-mixed layer from the balance between the kinetic turbulent energy induced by the wind and the buoyancy input by heating at the surface and the entrainment of heavy waters from below. The model is an adaptation of the formulation of Gill and Turner (1976) and is described *in extenso* in Staneva *et al.* (1998).

The 1-D BIOGEN model has been run as a closed system for several years until reaching a steady state for all state variables. This was generally achieved after less than 5-year-runs. The atmospheric forcing (heat flux and wind stress) was obtained from the climatological data set of Sorkina (1974), corrected by adding high frequency (twice daily) signals obtained from the US National Meteorological Centre for the period 1980–1986. Vertical discretization was 5 m and the sediment module was connected to the bottom layer.

Two sets of nutrient initial conditions were used in order to test the model's response in two 'water columns' representative of the surface open Black Sea (200 m deep), on the one hand, and of the shelf waters (40 m) under the influence of the Danube, on the other. Initial nutrient concentrations (Table 2) were chosen from data collected during the EROS 21 cruise of the RV *Professor Vodyanitsky* during the winter–spring transition period of 1997.

TABLE 2. 1-D BIOGEN: initial conditions for nutrient concentrations in the surface layer (source: cruise report of EROS 21, leg 1 of the RV *Professor Vodyanitsky*, 1997)

Nutrient (μM)	Open sea	Shelf area
NO_3	2·2	30·7
NH_4	0·2	1·2
PO_4	0·1	0·4
$Si(OH)_4$	5·5	21·5

0-D 1-D BIOGEN

The numerical frame consisted of the 'on-line' coupling of the 'open-sea' 1-D BIOGEN with a 'coastal' BIOGEN box model of variable volume. The former model represents the open-sea boundary conditions as described above. The box model symbolizes the coastal area influenced by freshwater and nutrient loads by the Danube River. Two fixed latitudes, the coast and a moving interface defined by a salinity of 17 determine its geographical limits. The volume of the coastal box and its exchange fluxes with the 'open-sea' water column were obtained at each time-step from the data diagnosed by the 3-D GHER general circulation model constrained by climatological atmospheric and freshwater (Altman & Kumish, 1986) forcing. The procedure is described *in extenso* in Beckers *et al.* (2002). In short, the average concentration of any biogeochemical variable C in the box model is calculated according to the following equation:

$$dC/dt = P^c + Q_r/V(C_r - C) + Q_1^{in}/V(C_1 - C) + Q_3^{in}/V(C_3 - C) + A/V(C_2 - C) \quad (1)$$

in which P^c results from the internal biogeochemical transformations of C calculated by the BIOGEN equations, Q_r is the Danube River input and Q_1^{in} and Q_3^{in} represent the north and south water inflow into box volume V, respectively. The coefficient A parameterizes the diffusion between the coastal and the open-sea boxes. C_2 is the open-sea surface layer concentration of C predicted by the 'open-sea' 1-D

BIOGEN model. C_1 and C_3 are the concentrations of the northern and southern boundaries of the box (equal to C or C_2 depending on the sign of Q_1^{in} and Q_3^{in}, respectively).

Q_3^{in}, Q_3^{in}, A, V and the average salinity S of the coastal box were calculated in the coupled model interactively at each time-step (1 h) from the 15-day data diagnosed by the circulation model of Beckers *et al.* (2000). A zero gradient condition was imposed for lateral ' open-sea ' boundary conditions of biogeochemical variables. River boundary conditions were restricted to inorganic nutrients. Hourly nutrient inputs by the Danube River were provided from the interpolation of monthly nutrient concentrations measured at the Danube mouth for the period 1980–1995 (Cociasu *et al.*, 1997) and the climatological freshwater discharges estimated by Altman and Kumish (1986). In such conditions, the mathematical tool is able to test the ecosystem response to changing nutrient concentrations without interfering with the interannual variations of atmospheric forcing.

Model results

Modelling seasonal physicochemical changes and biological successions in the stratified Black Sea water column: 1-D BIOGEN

The seasonal variation of the surface layer physical structure of the open Black Sea due to the climatological atmospheric forcing is illustrated in Figure 2 by the vertically resolved temperature [Figure 2(a)] and depth of the upper mixed layer [Figure 2(b)]. The simulated thickness of the upper mixed layer fluctuates between 5 and 60 m, which corresponds well with previous observations (Oguz *et al.*, 1996; Staneva *et al.*, 1998). Convective mixing is maximal at the end of February, deepening the mixed layer depth up to about 60 m [Figure 2(b)], with temperature characteristic of 6·5–7·0 °C [Figure 2(a)]. Deeper winter convection is prevented by the shallow, permanent pycnocline that characterizes the Black Sea. This feature results from the strong freshwater dilution of Black Sea surface waters and the inflow of denser Mediterranean Sea waters through the Bosphorus Strait. In spring, the water column warms up gradually and a strong thermocline is predicted at the base of a shallow, upper mixed layer in mid-summer [5–10 m; Figure 2(b)]. Accordingly, the maximum sea-surface temperature is observed during mid-summer and is about 24 °C [Figure 2(a)], in perfect agreement with observations recorded during the EROS 2000 cruises of July–August 1995 [e.g. Figure 5(b)] and by other (e.g. Vedernikov & Demidov, 1997).

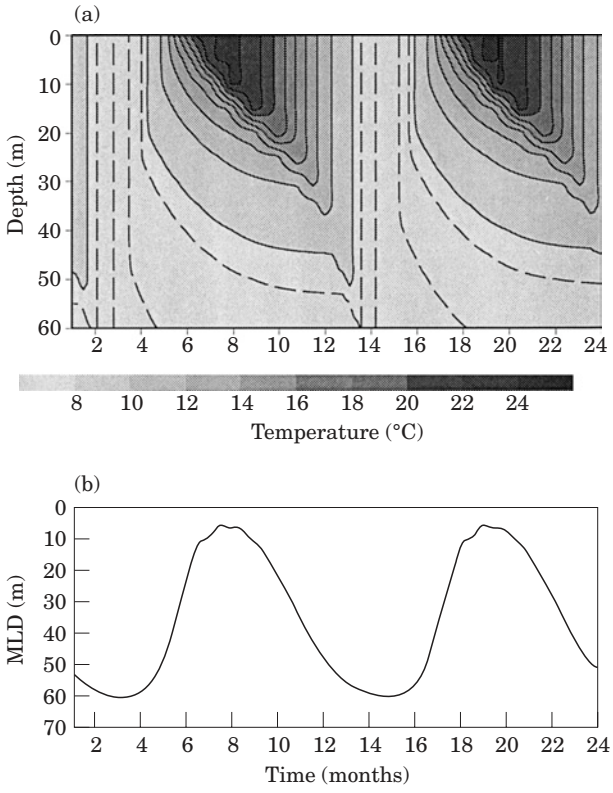

FIGURE 2. Two-year simulations of seasonal variations of (a) the vertical profiles of temperature and (b) the upper mixed layer depth.

Figures 3 and 4 show the steady-state time evolution of the vertical profiles of nutrients and biological state variables predicted for nutrient conditions mimicking the ' open area ' and ' shelf area ' water columns, respectively. The steep gradients simulated at 60 m and below (Figure 3) result from the Black Sea's strong stratification, which prevents the enrichment of surface layers with high concentrations of nutrients from deeper layers.

Reasonable agreement is observed between model predictions and data available for the central basin, both seasonally and in magnitude. As an example, Figure 5 compares selected vertical profiles of BIOGEN simulations and nutrients and chlorophyll *a* observations for spring [Figure 5(a)] and summer [Figure 5(b)] periods.

In accordance with the 1997 data (Ragueneau *et al.*, 2000), the predicted steady-state winter nutrient signature of the open Black Sea is ' silicate-excess ', but ' nitrogen- and phosphate-deficient ' compared to the Si/N/P molar ratio of 16:16:1, summarizing the stoichiometry of phytoplankton and diatoms (Redfield *et al.*, 1963; Brzezinski, 1985). Steady-state open-sea winter concentrations of nitrates [Figure 3(a)] are

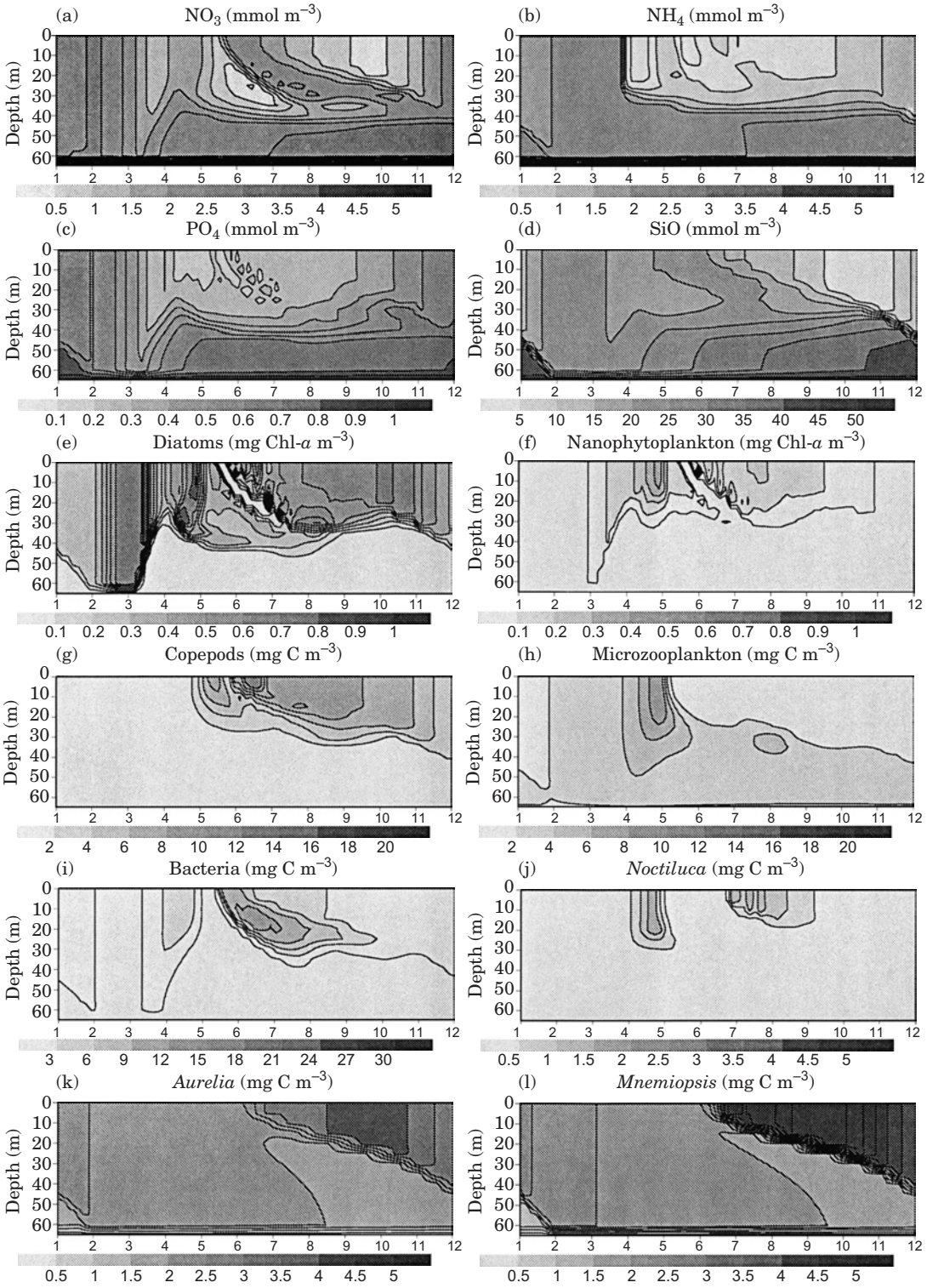

FIGURE 3. 1-D BIOGEN predictions in the open-sea water column of the Black Sea obtained after the fifth year-run: (a) nitrates; (b) ammonium; (c) phosphate; (d) silicate; (e) diatom–Chl *a*; (f) nanoflagellate–Chl *a*; (g) copepods; (h) microzooplankton; (i) bacteria; (j) *Noctiluca*; (k) *Aurelia*; (l) *Mnemiopsis*.

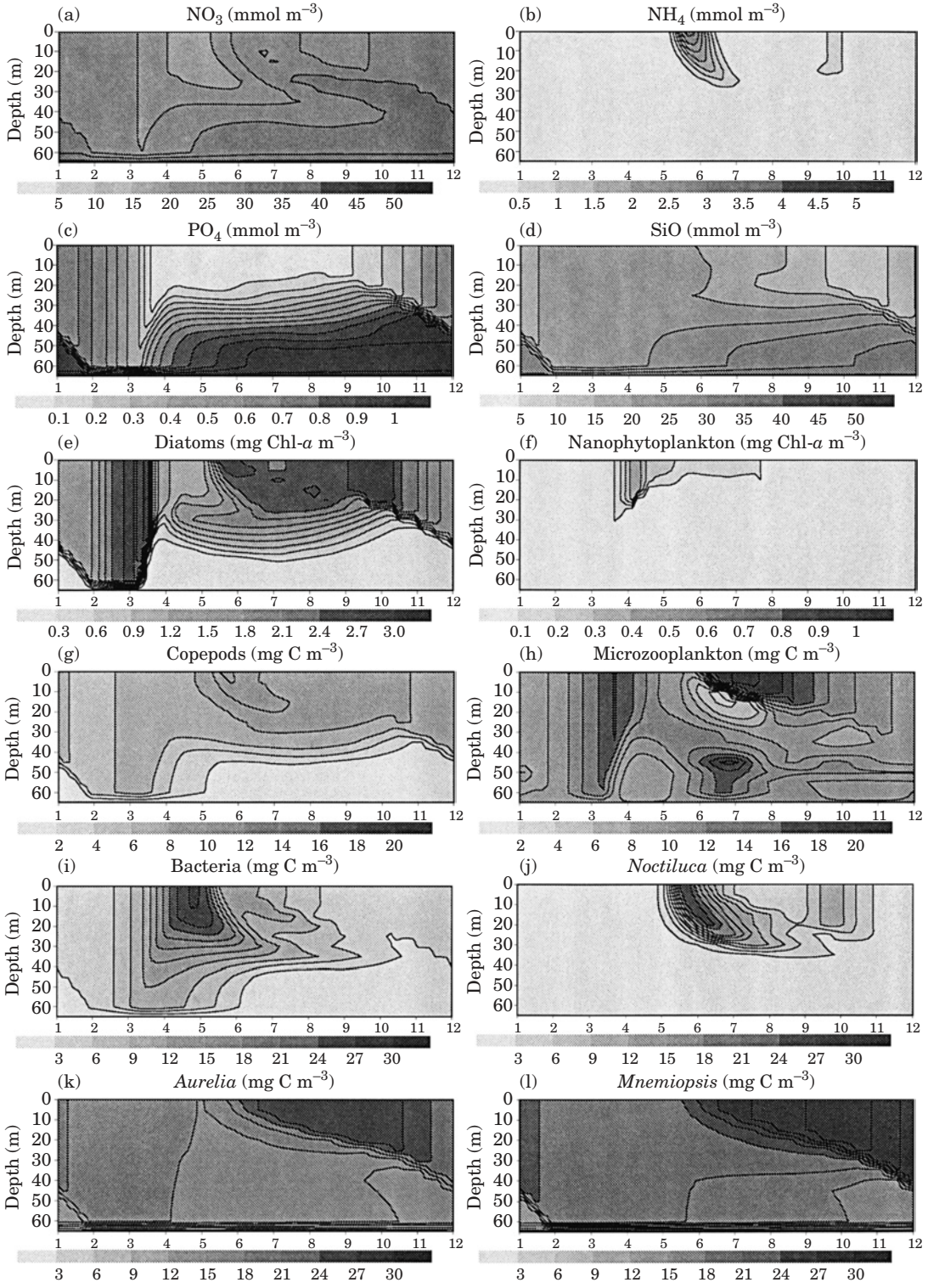

FIGURE 4. 1-D BIOGEN predictions in the nutrient-enriched water column obtained after the fifth year-run: (a) nitrates; (b) ammonium; (c) phosphate; (d) silicate; (e) diatom–Chl *a*; (f) nanoflagellate–Chl *a*; (g) copepods; (h) microzooplankton; (i) bacteria; (j) *Noctiluca*; (k) *Aurelia*; (l) *Mnemiopsis*.

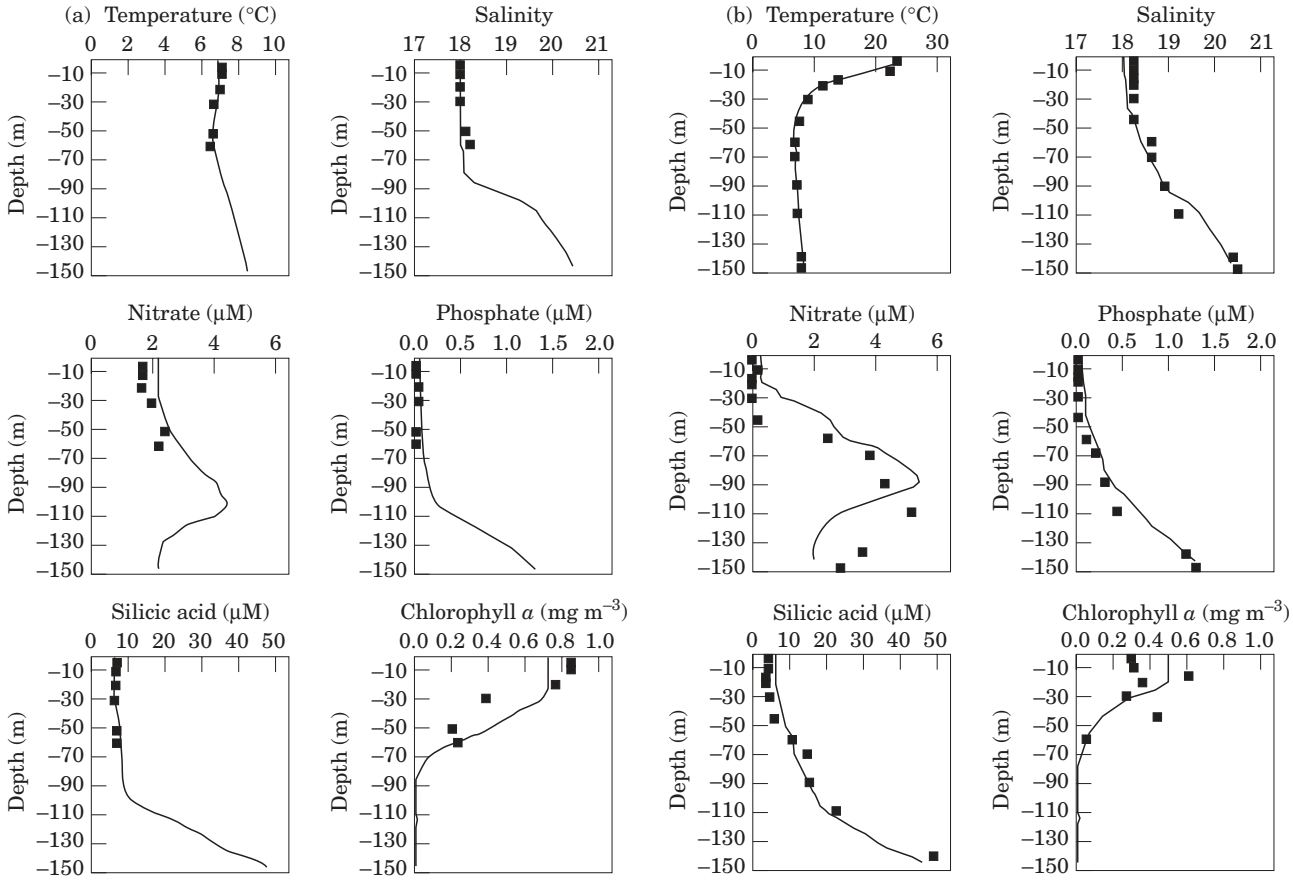

FIGURE 5. 1-D BIOGEN simulations in the open Black Sea water column. Observations recorded in (a) April 1997 and (b) July 1995. (■), data; (——), model.

typically those characteristic of the central basin (Konovalov, 1999). In contrast, simulated winter concentrations of phosphate, ammonium and silicic acid are slightly higher than generally observed. As expected in stratified marine systems in general and in the Black Sea in particular (Vedernikov & Demidov, 1997; Vinegradov *et al.*, 1999), the model simulates the development in mid-March of a phytoplankton spring bloom composed of diatoms [Figure 3(e)]. The onset of the spring diatom bloom corresponds to the installation of the thermocline at 35 m, when the surface layer temperature is about 8 °C (Figure 2). The bloom occupies the upper mixed layer and reaches a maximum of 1·2 mg Chl-*a* m^{-3} [Figure 3(e)], in fair agreement with observations [Figure 5(a); Vinegradov *et al.*, 1999]. Its magnitude is controlled by nutrient resources—nitrate [Figure 3(a)], but mostly phosphate [Figure 3(c)]—rather than by the grazing pressure of copepods, whose biomass remains at its lowest level until late April [Figure 3(g)]. As a result, significant concentrations of silicate [5–10 μM; Figures 3(d) and 5(a)] are leftover at the decline of early spring diatoms. The disappearance of early April diatoms, either because of their autolysis or sedimentation, releases dissolved and particulate organic matter (not shown) into the water column, which in turn stimulate the growth of bacteria. The latter reach a biomass of 10 mg C m^{-3} approximately, 10 days after the spring diatom bloom [Figure 3k,e]. This delay is explained by the macromolecular structure of diatom-derived substrates that have to be hydrolysed in monomers prior to being taken up by bacteria (see equations in Appendix). Based on regenerated nitrogen and phosphorus associated with the bacterial degradation of ungrazed spring diatoms, the model predicts a cascade of auto- and heterotrophic successions of low amplitude in April–May (Figure 3). Firstly, a rather modest surface layer phytoplankton bloom, almost equally composed of diatoms [$\sim$0·6 mg Chl-*a* m^{-3}; Figure 3(g)] and nanophytoflagellates [$\sim$0·4 mg Chl-*a* m^{-3}; Figure 3(f)], is simulated in early May. The amplitude of these blooms is regulated by phosphate availability and by the pressure of their respective grazers; the

copepods, whose grazing activity on diatoms is stimulated by the higher temperature in May [Figure 3(g)], and the ubiquitous microzooplankton [Figure 3(h)]. Interestingly, model simulations show a response delay between copepods and diatoms [Figure 3(e,g)], and a strong coupling between microzooplankton and nanophytoplankton, which peak almost synchronously [Figure 3(f,h)]. In mid-May, the microzooplankton bloom is repressed by the grazing pressure of copepods that shift from diatoms to microzooplankton prey after the decline of the former[Figure 3(e,g,h)]. The predicted biomass of copepods [Figure 3(g)] reaches a maximum of about 14 mg C m^{-3} in June and exceeds that of the microzooplankton [Figure 3(h)]. The maximum biomass of copepods correlates with secondary diatom blooms sustained by regenerated phosphate [Figure 3(c,e,g)], as suggested by the short-term oscillations of the latter and its co-occurrence with high bacterial biomass [Figure 3(i)]. In such conditions of low phosphate availability, the simulated phosphate pattern of June–July could well reflect a competition between diatoms and bacteria for his essential nutrient.

Furthermore, several subsurface, summer diatom blooms are predicted [Figure 3(e)], supported by the supply of nutrient-rich waters from below under conditions of sufficient light. As observed by several authors (Sorokin, 1982; Vedernikov & Demidov, 1997; Vinogradov *et al.*, 1999), an autumn diatom bloom of $\sim 0{\cdot}7$ mg Chl-*a* m^{-3} is predicted and corresponds to the increased vertical mixing with nutrient-rich deeper waters [Figure 2(b)]. In contrast with early spring, the autumn diatom bloom sustains some copepod growth [Figure 3(e,g)]. The simulated biomass of all gelatinous organisms—*Noctiluca*, *Aurelia*, *Mnemiopsis*—is not very significant [less than 5 mg C m^{-3}; Figure 3(j,k,l)] due to the low concentration of their food resources in comparison with their needs. *Noctiluca* peak in May and July–august when microzooplankton and/or nanophytoplankton are abundant [Figure 3(f,h,j)]. *Aurelia* and *Mnemiopsis* develop in late summer–early autumn when copepods reach their maximum biomass [Figure 3(g,k,l)]. The predicted biomass of both gelatinous carnivores is a factor of two lower compared to observations in 1992 (Vinogradov *et al.*, 1999).

In summary, 1-D BIOGEN simulations in the open Black Sea indicate that the surface layer planktonic system is driven by winter phosphate availability, which determines the magnitude and extent of the early spring diatom bloom. The mismatch predicted between early spring diatoms and copepod grazing limited by low temperature is, via the microbial degradation of organic matter derived from ungrazed diatoms, at the basis of a complex nutrient-regenerating food-web with strong interactions. As expected in summer in oceanic waters, this food-web includes an active microbial network (bacteria, nanophytoplankton and microzooplankton) in addition to diatoms and copepods. In this silicon-excess system, the summer blooms of diatoms are regulated by phosphate availability. The success of copepods in summer–autumn is explained by their ability to switch from diatoms to microzooplankton prey and vice versa, as well as by the lack of control by food-limited gelatinous carnivores. Finally, it must be stressed that the predicted silicate never reached a limiting level and was always higher than predicted nitrates, which is consistent with observations (Konovalov, 1999; Figure 5).

BIOGEN predictions in the ‘Danube-influenced shelf’ water column, mimicking the 1997 nutrient conditions (Figure 4), show a quite different steady-state winter nutrient regime due to the different signatures of river and marine waters. Steady-state winter concentrations are strongly enriched in nitrogen and phosphate and show an excess of nitrate with respect to silicon and phosphorus when compared to the phytoplankton stoichiometry [Figure 4(a,b,c,d)]. As in the open Black Sea, a diatom bloom is simulated in early March, but is three times higher in biomass [Figure 4(e)]. Again, this early spring diatom bloom is severely limited by ambient phosphate [Figure 4(c,e)] and is apparently poorly grazed by copepods, whose biomass is at its lowest level, although still more than twice that of the open Black Sea [Figures 4(g) and 3(g)]. Furthermore, the bacterial regeneration processes associated to the degradation of ungrazed diatoms stimulate an active microbial network, with bacteria and microzooplankton reaching a significantly higher biomass compared to copepods [Figure 4(g,h)] and to similar predictions in the open Black Sea [Figure 3(g,h)]. Although not directly comparable, these simulations are qualitatively and quantitatively supported by the 1995 microbiological observations in the north-western Black Sea (Bouvier, 1998). Model predictions show two peaks of microzooplankton separated by a huge bloom of *Noctiluca* lasting from mid-May to the end of June [Figure 4(l)]. The maximum biomass simulated [~ 30 mg C m^{-3}; Figure 4(j)] is higher by far than that of copepods and microzooplankton, and equivalent to bacteria, all in perfect agreement with 1995 observations (Bouvier, 1998; Weisse *et al.*, 2002). At this time, the water column is literally cleaned of other micro-organisms (Figure 4), which is explained by the voracious feeding of this omnivorous gelatinous dinoflagellate. In the absence of significant phytoplankton biomass, a

transient accumulation of the ammonium released by *Noctiluca* catabolic losses is predicted at *Noctiluca* maximal biomass [Figure 4(b,e,f,j)]. Such an accumulation is not simulated for phosphate due to the strong limitation of this nutrient. Compared to the open Black Sea simulations, where carnivorous gelatinous organisms were quasi-absent [Figure 3(m,n)], significant biomasses of both *Aurelia* and *Mnemiopsis* are simulated in this nutrient-enriched water column over the whole season, but mostly during the summer–autumn period [Figure 4(m,n)].

In summary, model predictions clearly suggest that the unbalanced nutrient enrichment of the Black Sea, mimicking the 1997 situation, stimulates the diatom component of the phytoplankton community as long as phosphate is not limiting. The diatom–copepod linear food-chain is also enhanced, but its extent is controlled by the strong feeding pressure of the gelatinous carnivores, which maintains copepods at a biomass of between 5 and 10 mg C m^{-3}. Consequently, much of the diatom production is not grazed and a very active microbial network develops, sustained by organic matter derived from ungrazed diatoms. High biomass is predicted for all microorganisms that allow for the development of *Noctiluca* in an explosive way. Finally, it is interesting to note that the maximal biomass predicted for the different gelatinous organisms is quite similar—$\sim$30 mg C m^{-3}—although delayed in time [Figure 4(j,k,l)].

Modelling the response of the north-western Black Sea ecosystem to changes in nutrient delivery by the Danube River after its damming in 1972: coupling a 'Lagrangian-like' BIOGEN box model to 1-D BIOGEN

The previous comparative analysis of 1-D BIOGEN results, constrained by climatological atmospheric forcing and nutrient conditions mimicking those typical of the open Black Sea and the Danube–Black Sea mixing zone, indicates that this model is suitable for simulating the response of the coastal ecosystem to changing nutrient loads. The capability of the BIOGEN model to simulate the ecological changes taking place in the north-western Black Sea over the last decade in response to changing nutrient delivery by the Danube was further investigated. For this purpose, the coupled 'box-1-D-water-column' BIOGEN has been run under three contrasting nutrient loads by the River Danube, corresponding to the post-Danube damming by the Iron Gates (Table 1). This period was chosen because of the availability of the complete sets of nutrient concentrations at the Danube out-flow (Cociasu *et al.*, 1977). Before 1985, some nutrient forms were not measured.

Model results verification was first conducted in the Danube-Black Sea mixing zone by constraining the model with the Danube nutrient concentrations of 1995 (Figure 6). This year was chosen because field observations are available for most state variables, although they are restricted to the summer period when heterotrophs are reaching their maximum biomass [Figure 6(b)] and primary production is sustained by regenerated nutrients. Table 3 compares nutrient and biological data collected in the surface waters of the 12–17 salinity transition zone during leg 1 of the EROS 2000 cruise of the RV *Professor Vodyanitsky* in July 1995 and BIOGEN model results averaged over the 1-month cruise duration. Such a comparison was chosen due to the inherent difference between the cruise (grid along eutroph–oligotroph gradients) and model (homogeneous box) sampling mode. Examination of Table 3 shows a reasonable correlation between predictions and observations. As a general trend, however, predictions are closer to the corresponding minimal than average field values (Table 3). This is explained by the higher average salinity of the field grid compared to that of the box model (Table 3). From this it can be concluded that model runs with the coupled 'box-1-D-water-column' BIOGEN are simulating chemical and ecological changes close to the frontal area between the Danube and the open water.

Figure 6 compares the seasonal predictions of nutrients and biological variables in the Danube–Black Sea mixing zone obtained by running the coupled 'box-1-D-water-column' BIOGEN under the forcing of the Danube nutrient loads of 1985, 1991 and 1995 [Figure 6(a); Cociasu *et al.*, 1997]. A significant interannual and seasonal variability of Danube nutrient concentrations distinguishes these three years [Figure 6(a)]. The fluctuations reflect human-induced changes in the Danube watershed and/or different biogeochemical transformations in the river system (Garnier *et al.*, 2002). This had dramatic results for nutrient concentrations at the Danube out-flow in the Black Sea, which were modified both quantitatively and qualitatively [Figure 6(a)]. Phosphate was the most changeable nutrient, peaking at tremendously high concentrations in 1991 [Figure 6(a)]. As a general trend, nitrate and phosphate Danube concentrations in 1995 were at their lowest level for this 'post-Iron Gates' period. No real trend can be concluded from silic acid fluctuations shown by Figure 6(a), although river loads of silicon have been reported to decrease after the Danube damming (Humborg *et al.*, 1997). BIOGEN

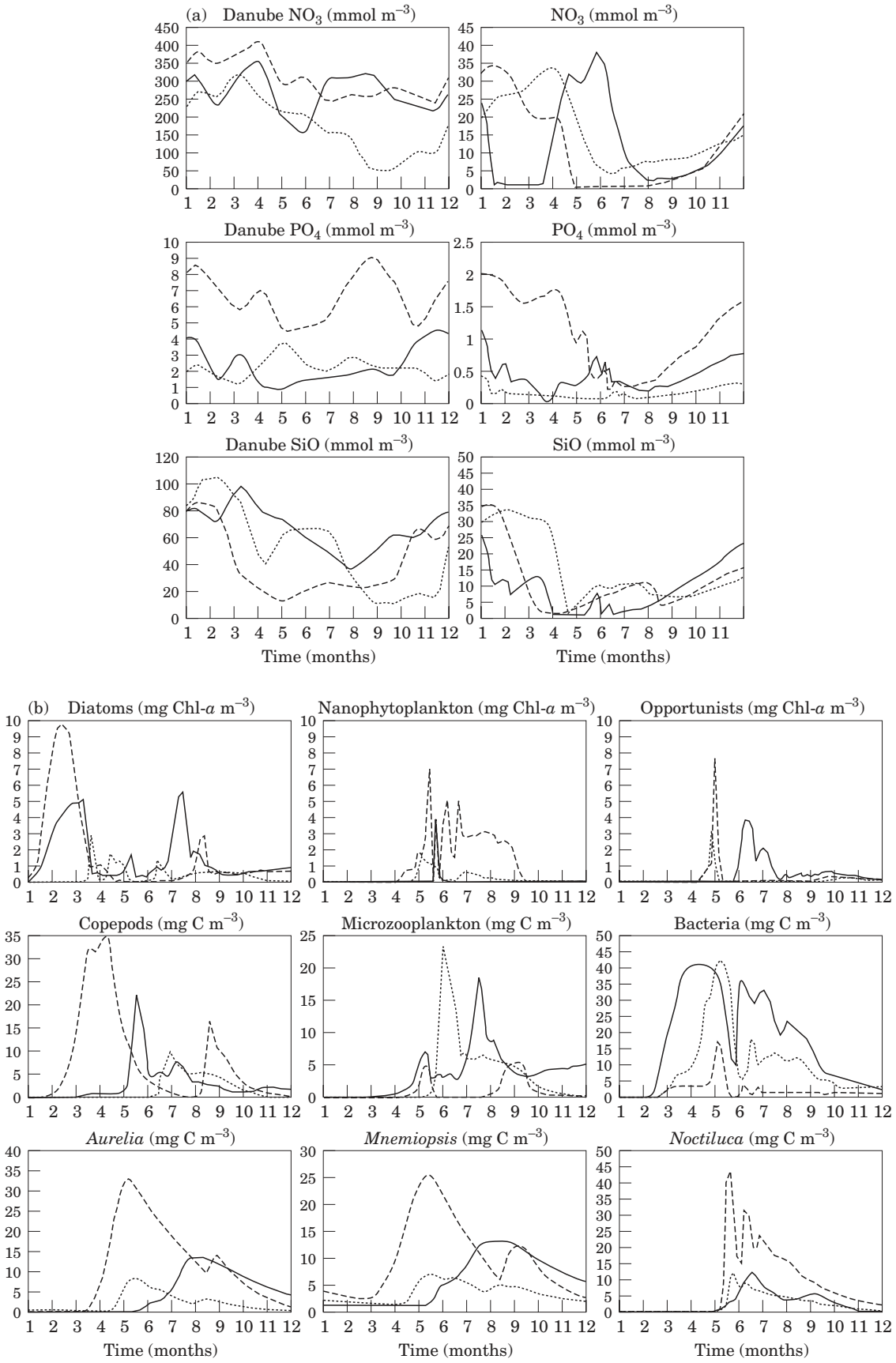

FIGURE 6. Time evolution of (a) Danube nutrient forcing and corresponding 0–1-D BIOGEN nutrient simulations in the Danube–Black Sea mixing zone and (b) 0–1-D BIOGEN predictions of nutrients and biological state variables in the Danube–Black Sea mixing zone. (——), 1985; (– – –), 1991; (· · ·), 1995.

TABLE 3. Comparison between model predictions in the Danube–Black Sea mixing zone and data collected during the EROS 2000, leg 1 cruise of the RV *Professor Vodyanitsky*, in July 1995

State variable	Field data			BIOGEN
	Mean	Min.	Max.	
Salinity	14·52	12·55	16·59	15·7
NO_3[a] (μM)	2·54	0·0	15·32	5·9
NH_4[b] (μM)	0·87	0·24	2·42	1·53
PO_4[c] (μM)	0·14	0·10	0·4	0·15
$Si(OH)_4$[d] (μM)	5·33	1·96	12·41	8·89
Phytoplankton[e] (mg Chl *a* m^{-3})	3·42	0·47	6·28	1·44
Microzooplankton[c] (mg C m^{-3})	115·2	9·11	224·6	12·35
Bacteria[f] (mg C m^{-3})	34·68	11·1	53·9	18·3
Copepods[g] (mg C m^{-3})	8·62			6·94
Noctiluca[g] (mg C m^{-3})	8·37			6·31

[a]A. Krastev (in EROS cruise report, 1995); [b]J. Vervlimmeren (in EROS cruise report, 1995); [c]R. Pencheva (in EROS cruise report, 1995); [d]L. Popa (in EROS cruise report, 1995); [e]S. Moncheva (in EROS cruise report, 1995); [f]T. Bouvier (1998); [g]B. Alexandrov, T. Weisse and U. Scheffel (unpubl. data).

simulations in the Danube–Black Sea mixing zone reproduce the observed interannual variability of winter concentrations of nitrates and phosphates in the Danube [Figure 6(a)]. However, due to mixing with silicate-rich marine waters, the predicted winter nutrient balance is significantly different from that of the river [Figure 6(a)]. Consequently, a higher winter stock of nutrients is predicted in the Danube–Black Sea mixing zone in 1991 compared to 1985 and 1995. Moreover, the simulated winter nutrients of 1991 are relatively well balanced with respect to coastal diatom and phytoplankton stoichiometry [Figure 6(a)]. Predicted winter concentrations of nitrates and silicate are very comparable in 1985 and 1995. Interestingly, the model predicts severe phosphate depletion in 1995 [Figure 6(a)]. Nutrient simulations in the Danube–Black Sea mixing zone show similar seasonal fluctuations between years with the lowest values occurring in the spring–summer period due to biological uptake [Figure 6(a,b)]. However, the simulated delay of the nutrient spring decreases suggests, in conditions of climatological atmospheric forcing, a very sensitive response from the phytoplankton community and related heterotrophs to changing nutrients. Accordingly, contrasting phytoplankton and heterotrophc successions are simulated for the three different years [Figure 6(b)]. As a general trend, a well-balanced nutrient enrichment, such as that of 1991, is shown to stimulate the growth of all components of the phytoplankton community [Figure 6(b)]. The most visible effect on the planktonic food-chain is the enhancement in early spring to its linear branch composed of diatoms and copepods, the latter blooming after the diatoms following a 1 month delay [Figure 6(b)]. Moreover, these nutrient-rich conditions also stimulate the gelatinous organisms—*Noctiluca*, *Aurelia*, *Mnemiopsis*—which reach, in summer, a predicted biomass level similar to that of the copepods [Figure 6(b)]. In contrast, the model predicts little development of the microbial network composed of bacteria and microzooplankton, allowing nanophytoplankton to reach a non-negligible biomass that persists during the whole vegetative period [Figure 6(b)]. On the other hand, the phosphate-deficient nutrient conditions in 1985 and 1995 are predicted to enhance the microbial network relative to the linear food-chain and as much as phosphate is strongly depleted [Figure 6(b)]. Bacteria, in particular, reach a tremendously high biomass and appear to play a key role in phosphate regeneration processes. Incidentally, such high bacterial biomass was measured during the 1995 EROS 2000 cruise (Bouvier, 1998). A lower biomass of gelatinous carnivores is simulated in 1985 and 1995 compared to levels in 1991, which corresponds with a lower simulated copepod biomass [Figure 6(b)]. Also, in 1985 and 1995, the predicted biomass of *Noctiluca* is significantly lower than in 1991. Although the simulated *Noctiluca* biomass is similar for both years, the model predicts a 1-month shift in their maxima, with *Noctiluca* blooming in mid-June and mid-July in 1995 and 1985, respectively. As a general trend, the model predicts a strong interannual variability in the timing of autotrophic and heterotrophic successions (Figure 6), largely driven by changing nutrients, since light and temperature conditions remain the same.

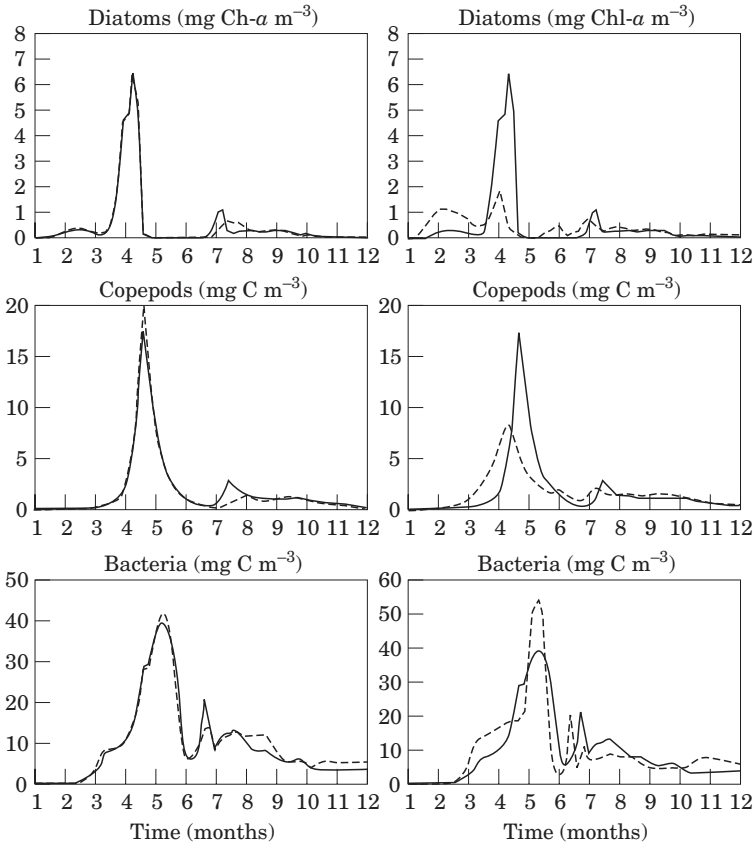

FIGURE 7. Sensitivity of the 0–1-D BIOGEN predictions for 1991 in the Danube–Black Sea mixing zone to the coefficients describing the exchanges between the coastal area and the adjacent zones. Left panel: sensitivity to the exchange coefficient between the coastal and open-sea areas; right panel: sensitivity to the southern and northern inflow fluxes.

Discussion

Sensitivity of the BIOGEN predictions to hydrodynamics

Prior to its further ' on-line ' coupling with a 3-D General Circulation Model of the Black Sea, the high-trophic resolution ecological model BIOGEN has been numerically implemented in the north-western Black Sea by coupling a 0-D ' Lagrangian-like ' BIOGEN box model subjected to the Danube with a 1-D BIOGEN representing the open-sea boundary conditions. The extent to which this aggregated and simplified representation of the complex hydrodynamics prevailing in this shelf area is realistic with respect to the eutrophication-related question addressed by the mathematical model has been investigated by conducting sensitivity studies of BIOGEN predictions to physical fluxes between the Danube–Black Sea mixing zone and the adjacent open-sea areas. Figure 7 shows BIOGEN simulations of three key biological state variables obtained when changing (1) the exchange coefficient between the shelf box and the open-sea water column (Figure 7, left panel) and (2) the water inflow from the north and south, taking the mixing coefficients that specify the errors in estimating the fluxes into consideration (Figure 7, right panel). The exchange coefficients and fluxes, and their sensitivity to the physical state variables, are described *in extenso* in Beckers *et al.* (2002). Comparing these simulations with those obtained by changing Danube nutrient loads (Figure 6) suggests little sensitivity of BIOGEN predictions to the parameterization of the exchange coefficient between the shelf and open areas. This indicates that the current numerical implementation can be used as a first approach to explore the response of the north-western Black Sea ecosystem to changes in Danube nutrient delivery. Higher sensitivity of BIOGEN predictions is, however, obtained by changing the mixing of inflowing waters (Figure 7). This suggests that the inflow conditions from the Rim current have a marked influence on the ecosystem dynamics of the Danube–Black Sea mixing zone, bordered at a salinity of 17. Interestingly, however, the changing inflow conditions mainly affect the magnitude of the state variables, with little effect on their

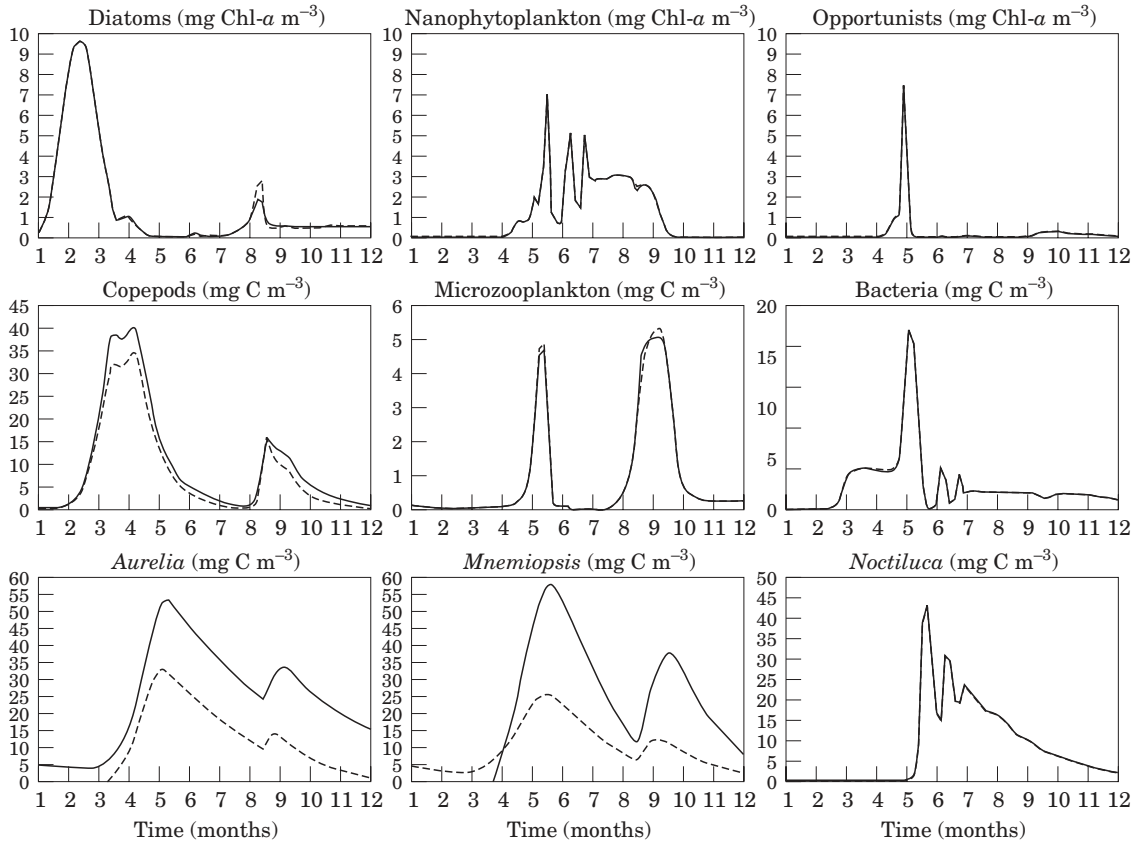

FIGURE 8. Sensitivity of the 1991 BIOGEN predictions to fishing pressure obtained indirectly by changing copepod mortality to fish predation. (– – –), current 1991 prediction; (——), twofold decrease of copepod mortality by fish pressure.

time evolution (Figure 7, right panel). In contrast, changing the Danube nutrient inputs to the Black Sea over the season has a marked incidence on the magnitude, bloom extent and time appearance of all biological state variables (Figure 7). This difference is consistent with the chosen proportional change of inflow conditions. Further implementation of BIOGEN in a high-resolution 3-D model of the shelf dynamics, nested into the GHER general circulation model of the Black Sea (Beckers *et al.*, 2002), would provide an accurate estimation of the combined influence of the Danube and the Rim current on the structure and functioning of the north-western Black Sea shelf ecosystem.

Nutrient changes and trophic structures

Model scenarios of changing Danube nutrient inputs to the north-western Black Sea observed over the 1985–1995 period show that the mechanistic BIOGEN model, based on food-chain structure and physiological concepts, has the required trophic resolution to address the ecological changes evident in the Black Sea since the 1960s. Model result analyses indicate that coastal eutrophicated-related problems are not only driven by the quantity of nutrients discharged into the coastal system, but that the balance between them is just as important. BIOGEN predictions clearly demonstrate that limiting nutrients determines the structure of the phytoplankton community, which in turn constrains the structure and functioning of the planktonic food-web. In particular, it shows that a well-balanced N:P:Si nutrient enrichment, as observed, for example, in 1991, has a positive effect on the diatom–copepod linear food-chain, while the regenerated-based microbial food-chain remains at its basic level. When present in the system, gelatinous carnivores also benefit from this enrichment through their feeding on the increased copepod biomass. Nitrogen or phosphate limitation, on the other hand, directs the structure of the planktonic food-web towards the dominance of an active microbial food-web in which bacteria and microzooplankton play a key role; the former as nutrient regenerator, the latter as a trophic path to the copepods and hence to the linear food-chain. In the typically ‘ silicate-excess ’

Black Sea ecosystem, phosphate rather than nitrogen constrains the structure and functioning of the Black Sea ecosystem. Hence, the successful development of gelatinous carnivores is inversely correlated to phosphate limitation. Therefore, the observed positive signs of recovery of the Black Sea ecosystem (Lancelot *et al.*, 1998) might well be related to the reduction of nutrient loads in particular phosphate, by the Danube.

More generally, model results indicate that the current concept of diatoms as better competitors for inorganic nitrogen and phosphate when there is sufficient silicon—the general concept behind the current understanding of anthropogenic eutrophication—does not hold. BIOGEN predictions, in agreement with recent field observations (Ragueneau *et al.*, 2002), clearly suggest that diatom growth in the coastal and open Black Sea has been regulated over the last decade by ambient phosphate in spring and nitrogen and phosphate in summer; with silicon never depleted. This contrasts with the current understanding of the eutrophication phenomenon of the Black Sea attributed to a combination of a concomitant increase in nitrogen but mostly phosphorus riverine loads and a decrease in silicate delivery (Cociasu *et al.*, 1997), the latter of which is attributed to the Danube damming in 1972 (Humborg *et al.*, 1997).

Eutrophication, fishing pressure and trophic structures

The BIOGEN model has further been used to test the recent hypothesis of Gücü (1997, 2002) on the crucial role of overfishing rather than man-made eutrophication as being responsible for the successful development of gelatinous carnivores in the north-western Black Sea in the late 1980s–early 1990s. The influence of the fisheries industry on the blooming of gelatinous carnivores was tested by running BIOGEN with the Danube nutrient loads of 1991 and changing the fishing coefficient. The latter was indirectly considered by modifying the first-order mortality coefficient of copepods, where a lower value corresponds to a higher fish pressure. Model simulations (Figure 8) suggests, under conditions of well-balanced nutrient enrichment, a positive link between fishing pressure and gelatinous carnivores. A greater than two-fold increase of the biomass of both carnivorous gelatinous organisms is predicted for a doubling of fishing pressure (Figure 8). Interestingly, no change is predicted among the whole auto- and heterotrophic community (Figure 8). Together, this first assay suggests that overfishing, in addition to eutrophication, could have played a role in the destabilization of the Black Sea ecosystem reported for the years 1989–1991. This demonstrates the capability of mechanistic models to handle the complex and non-linear nature of the link between human activities and the functioning of the Black Sea ecosystem.

Acknowledgements

This work is a contribution to the EROS 21 project funded by the programmes Environment and Climate (contract no. ENV4-CT96-0286) and INCO-Copernicus (contract IC20-CT96-0065) of the European Commission. It is publication no. 185 of the ELOISE initiative. The authors would like to thank Dr J.-M. Martin, Prof. N. Panin and Prof. V. Egorov, whose dedication has made the collaboration between Western and Eastern European institutions a successful one. We are grateful to T. Weisse and B. Alexandrov for helpful discussions about the parameterization of zooplankton feeding. Our thanks to T. Bouvier, A. Cociasu, A. Krastev, S. Moncheva, R. Pencheva, L. Popa and U. Scheffel for providing field data. Finally, we thank two anonymous reviewers for their critical and constructive comments.

References

Altman, E. N. & Kumish, N. I. 1986 Interannual and seasonal variability of the Black Sea freshwater balance. *Trydi Gosudarstvenae Oceanographicheskogo Institute* **145,** 3–15 (in Russian).

Beckers, J.-M., Gregoire, M., Nihoul, J. C. J., Stanev, E., Staneva, J. & Lancelot, C. 2002 Modelling the Danube-influenced north-western continental shelf of the Black Sea. I: Hydrodynamical processes simulated by 3-D and box models. *Estuarine, Coastal and Shelf Science* **54,** 453–472.

Billen, G. & Servais, P. 1989 Modélisation des processus de dégradation bactérienne de la matière organique en milieu acquatique. In *Micro-organismes dans les Écosystémes Océaniques* (Bianchi, M., Marty, D., Bertrand, J.-C., Caumette, P. & Gauthier, M.). Paris, Masson, pp. 219–245.

Billen, G., Dessery, S., Lancelot, C. & Meybeck, M. 1989 Seasonal and inter-annual variations of nitrogen diagenesis in the sediments of a recently impounded basin. *Biogeochemistry* **8,** 73–100.

Bingel, F., Kideys, A., Ozsoy, E., Turgul, S., Basturk, O. & Oguz, T. 1993 Stock assessment studies for the Turkish Black Sea coast. *NATO-TU Fisheries Final Report*. IMS, METU, 108 pp.

Bodeanu, N. 1992 Algal blooms and development of the main phytoplanktonic species at the Romanian Black Sea littoral in conditions of intensification of the eutrophication process. In *Marine Coastal Eutrophication: The Response of Marine Transitional Systems to Human Impact. Problems and Perspectives for Restoration* (Vollenweider, R. A., Marchetti, R. & Viviani, R., eds). *Science of the Total Environment* **Suppl. 1992,** 891–906.

Bologa, A. S., Skolka, H. V. & Frangopol, P. T. 1984 Annual cycle of planktonic primary productivity off the Romanian Black Sea. *Marine Ecology Progress Series* **19,** 25–32.

Bologa, A. S., Bodeanu, N., Petran, A., Tiganus, V. & Zaitsev, Y. 1995 Major modifications of the Black Sea benthic and planktonic biota in the last three decades. *Bulletin de l'Institut Océanographique de Monaco* **15,** 85–110.

Bondar, C. 1977 Changes in hydrological pattern induced by engineering works on the lower Danube. *Hidrotecnica* **22**, 87–89.

Bouvier, T. 1998 Structure et dynamique du réseau trophique microbien dans le bassin nord occidental de la Mer Noire sous influence du Danube. Ph.D. Dissertation, Université Libre de Bruxelles, Belgium.

Brzezinsky, A. M. 1985 The Si:C:N ratio of marine diatoms: interspecific variability and the effect of some environmental variables. *Journal of Phycology* **2,** 347–357.

Cokasar, T. & Özsoy, E. 1998 Comparative analysis and modelling for regional ecosystems of the Black Sea. In *Proceedings of the Symposium on the scientific results of the NATO-TU Black Sea Projects* (Oguz, T. & Ivanov, L., eds). NATO-ASI, Kluwer Academic Publisher, pp. 323–359.

Cociasu, A., Diaconu, V., Popa, L., Nae, I., Dorogan, L. & Malciu, V. 1997 The nutrient stock of the Romanian Shelf of the Black Sea during the last three decades. In *Sensitivity to Change: Black Sea, Baltic Sea and North Sea* (Ozsoy, E. & Mikaelyan, A., eds). *NATO ASI Series, 2—Environment* **27,** 49–65.

Garnier, J., Billen, G., Hannon, E., Fonbonne, S., Videdina, Y. & Soulie, M. 2002 Modelling the transfer and retention of nutrients in the drainage network of the Danube River. *Estuarine, Coastal and Shelf Science* **54,** 285–308.

Gill, A. & Turner, J. S. 1976 A comparison of seasonal thermocline models with observations. *Deep Sea Research* **21,** 391–401.

Gomoiu, M. T. 1990 Marine eutrophication syndrome in the north-western part of the Black Sea. In *Marine Coastal Eutrophication: The Response of Marine Transitional Systems to Human Impact. Problems and Perspectives for Restoration* (Vollenweider, R. A., Marchetti, R. & Viviani, R., eds) *Science of the Total Environment* **Suppl. 1992,** 683–703.

Grégoire, M., Beckers, J.-M., Nihoul, C. J. C. & Stanev, E. 1998 Reconnaissance of the main Black Sea's ecohydrodynamics by means of a 3-D interdisciplinary model. *Journal of Marine Systems* **16,** 85–105.

Gücü, A. C. 1997 Role of fishing in the Black Sea ecosystem. In *Sensitivity to Change: Black Sea and North Sea* (Ozsoy, E. & Mikaelyan, A., eds) *NATO ASI Series, 2—Environment* **27,** 149–162.

Gücü, A. C. 2002 Can overfishing be responsible for the successful establishment of *Mnemiapsis leidyi* in the Black Sea? *Estuarine, Coastal and Shelf Science* **54,** 439–451.

Hoffmeyer, M. S. 1990 Alganus observaciones sobre la alimentation de *Mnemiopsis mccradyi* Mayer, 1990 (Ctenophora, Lobata). *Set. Zool. Porto Alegre* **70,** 55–65.

Humborg, C. 1997 Primary productivity regime and nutrient removal in the Danube Estuary. *Estuarine, Coastal and Shelf Science* **45,** 579–589.

Humborg, C., Ittekkot, V., Cociasu, A. & Bodungen, B. 1997 Effect of Danube River dam on Black Sea biogeochemistry and ecosystem structure. *Nature* **386,** 385–388.

Ivanov, L. & Beverton, R. J. H. 1985 The fisheries resources of the Mediterranean. Part 2: Black Sea. G.F.C.M. *Studies and Reviews* **60,** FAO, Rome, 135 pp.

Konovalov, S. K., Ivanov, L. I., Murray, J. W. & Eremeeva, L. V. 1999 Eutrophication: a plausible cause for changes in hydrochemical structure of the Black Sea anoxic layer. In *Environmental Degradation of the Black Sea: Challenges and Remedies* (Besiktepe, S. T., Unlüata, U. & Bologa, A. S., eds) *NATO Science Series, 2—Environmental Security* **56,** 61–74.

Lancelot, C., Veth, C. & Mathot, S. 1991 Modelling ice-edge phytoplankton bloom in the Scotia–Weddell Sea sector of the Southern Ocean during spring 1988. *Journal of Marine Systems* **2,** 333–346.

Lancelot, C., Panin, N. & Martin, J.-M. 1998 The north-western Black Sea: a pilot site to understand the complex interaction between human activities and the coastal environment. In (Barthel, K.-G., Barth, H., Bohle-Carbonell, M., Fragakis, C., Lipiatou, E., Martin, P., Ollier, G. & Weydert, M., eds). *Third European Marine Science and Technology Conference—Project Synopsis, Vol. II: Strategic Marine Research,* European Commission (Luxembourg) EUR 18220 EN, pp. 706–713.

Lancelot, C., Rousseau, V., Billen, G. & Van Eeckhout, D. 1997*a* Coastal eutrophication of the Southern Bight of the North Sea: assessment and modelling. In *Sensitivity to Change: Black Sea, Baltic Sea and North Sea* (Ozsoy, E. & Mikaelyan, A., eds). *NATO ASI Series, 2—Environment* **27,** 439–454.

Lancelot, C., Becquevort, S., Menon, P., Mathot, S. & Dandois, J.-M. 1997*b* Ecological modelling of the planktonic microbial food-web. In *Belgian Research Programme on the Antarctic, Scientific Results of Phase III (1992–1996)* (Caschetto, S., ed.) **1,** 1–78.

Lancelot, C., Hannon, E., Becquevort, S., Veth, C. & de Baar, H. J. W. 2000 Modeling phytoplankton blooms and carbon export production in the Southern Ocean: Dominant controls by light and iron of the Atlantic sector in Autral spring 1992. *Deep Sea Research I* **47,** 1621–1662.

Masaryk, T. G. & Varley, I. 1997 Nutrient balances for Danube countries. *Danube Applied Research Program (95-0614.00, PHARE: ZZ911/0102), Final Report.* 98 pp.

Mee, L. D. 1992 The Black Sea in crisis: a need for concerted international action. *Ambio* **21,** 278–286.

Mutlu, E., Bingel, F., Gücü, A. C., Melnikov, V. V., Nierman, U., Ostr, N. A. & Zaika, V. E. 1994 Distribution of the new invader *Mnemiopsis* sp. and the resident *Aurelia aurita* and *Pleurobrachia pileus* populations in the Black Sea in the years 1991–1993. *ICES Journal of Marine Sciences* **51,** 407–421.

Oguz, T., Ducklow, H., Malanote-Rizzoli, P., Turgul, S., Nezlin, N. & Unluata, U. 1996 Simulation of annual plankton cycle in the Black Sea by a one-dimensional physical biological model. *Journal of Geophysical Research* **101,** 16551–16569.

Popa, A. 1993 Liquid and sediment inputs of the Danube River into the north-western Black Sea. In *Transport of Carbon and Nutrients in Lakes and Estuaries*, Part 6. SCOPE/UNEP Sonderband, pp. 137–149.

Porumb, F. 1989 On the development of *Noctiluca Scintillans* under eutrophication of Romanian Black Sea coastal waters. In *Marine Coastal Eutrophication: the Response of Marine Transitional Systems to Human Impact. Problems and Perspectives for Restoration* (Vollenweider, R. A., Marchetti, R. & Viviani, R., eds). *Science of the Total Environment* **Suppl. 1992,** 907–920.

Ragueneau, O., Egorov, V., Vervlimmeren, J., Cociasu, A., Déliat, G., Krastev, A., Daoud, N., Rousseau, V., Popovitchev, W., Brion, N., Popa, L., Gauwet, G. & Lancelot, C. 2002 Biogeochemical transformations of inorganic nutrients in the mixing zone between the Danube River and the north-western Black Sea. *Estuarine, Coastal and Shelf Science* **54,** 321–336.

Redfield, A. C., Ketchum, B. H. & Richards, F. A. 1963 The influence of organisms on the composition of sea water. In *The Sea* Vol. II (Hill, M. N., ed.). John Wiley, New York, pp. 26–77.

Shiganova, T. A. 1997 *Mnemiopsis Leidyi* abundance in the Black Sea and its impact on the pelagic community. In *Sensitivity to Change: Black Sea, Baltic Sea and North Sea* (Ozsoy, E. & Mikaelyan, A., eds). *NATO ASI Series, 2—Environment* **27,** 117–131.

Sorkina, A. I. 1974 *Reference Book on the Black Sea Climate*. Gydrometeoizdat, Moscow, 406 pp. (in Russian).

Sorokin, Yu. I. 1982 *The Black Sea*. Moscow, 216–pp.

Staneva, J. V., Stanev, E. V. & Oguz, T. 1998 The impact of atmospheric forcing and water column stratification on the yearly plankton cycle. In *Proceedings of the Symposium on the Scientific Results of the NATO-TU-Black Sea Project* (Oguz, T. & Ivanov, L., eds). *NATO-ASI Series,* 301–323.

Stepnowski, A., Gücü, A. C. & Bingel, F. 1993 Assessment of the pelagic fish resources in the southern Black Sea using echo integration and dual-beam processing. *Archives of Acoustics, Polish Academy of Science Journal* **18,** 83–104.

Tolmazin, D. 1985 Changing coastal oceanography of the Black Sea. *Progress in Oceanography* **15,** 217–276.

Van Eeckhourt, D. & Lancelot, C. 1997 Modelling the functioning of the north-western Black Sea ecosystem from 1960 to present.

In *Sensitivity to Change: Black Sea, Baltic Sea and North Sea* (Ozsoy, E. & Mikaelyan, A., eds). *NATO-ASI Series 2—Environment* **27,** 455–468.
Vedernikov, V. I. & Demidov, A. B. 1997 The vertical distribution of the primary production and chlorophyll in the different season of the deep parts of the Black Sea. *Oceanologya* **37,** 414–423.
Vinogradov, M. E. & Tumantseva, N. 1993 Some results of investigations of the Black Sea biologic communities. In *Black Sea Research Country Profiles (Level II)*. UNESCO, pp. 80–94.
Vinogradov, M. E., Shuskina, E. A., Mikaelyan, A. S. & Nezlin, N. P. 1999 Temporal (seasonal and interannual) changes of ecosystem of the open waters of the Black Sea. In *Environmental Degradation of the Black Sea: Challenges and Remedies* (Besiktepe, S. T., Unlüata, U. & Bologa, A. S., eds). *NATO Science Series, 2—Environmental Security* **56,** 109–129.
Weisse, T., Gomoiu, M.-T., Scheffel, U. & Brodrecht, F. 2002 Biomass and size composition of the comb jelly *Mnemiopsis* sp. in the north-western Black Sea during spring 1997 and summer 1995. *Estuarine, Coastal and Shelf Science* **54,** 423–437.
Zaitsev, Yu. P. 1993 Impacts of eutrophication on the Black Sea fauna: Studies and Reviews. *General Fisheries Council for the Mediterranean* **64,** 59–86.

Appendix

TABLE A1. The BIOGEN model: state variables

Variable	Symbol
Biological state variables:	
Diatoms: DA=DAF+DAS+DAR	
Functional and structural metabolites	DAF
Monomers	DAS
Reserves	DAR
Phototrophic nanoflagellates: NF=NFF+NFS+NFR	
Functional and structural metabolites	NFF
Monomers	NFS
Reserve products	NFR
Opportunistic phytoplankton: OP=OPF+OPS+OPR	
Functional and structural	OPF
Monomers	OPS
Reserve products	OPR
Bacteria	BAC
Microzooplankton	MCZ
Copepods	COP
Noctiluca	NOC
Aurelia aurita	AUR
Mnemiopsis sp.	MNE
Organic matter	
Monomeric: carbon, nitrogen	BSC, BSN
Dissolved polymers (high biodegradability): carbon, nitrogen, phosphorus	DC_1, DN_1, DP_1
Dissolved polymers (low biodegradability): carbon, nitrogen, phosphorus	DC_2, DN_2, DP_2
Particulate organic matter (high biodegradability): carbon, nitrogen, phosphorus	PC_1, PN_1, PP_1
Particulate organic matter (low biodegradability): carbon, nitrogen, phosphorus	PC_2, PN_2, PP_2
Detrital biogenic silica	BSi
Inorganic nutrients	
Nitrate	NO_3
Ammonium	NH_4
Phosphate	PO_4
Silicic acid	SiO

TABLE A2. The BIOGEN model: processes

Description	Symbol
Phytoplankton dynamics:	
Photosynthesis	φ_i i=DA, NF, OP
Growth	μ_i i=DA, NF, OP
Reserve synthesis	s_i i=DAR, NFR, OPR
Reserve catabolism	c_i i=DAR, NFR, OPR
Exudation	e_i i=DAS, NFS, OPS
Respiration	$resp_i$ i=DA, NF, OP
Autolysis	lys_{if} i=DA, NF, OP; j=F, S, R
Sedimentation	sed_{if} i=DA, OP; j=F, S, R
Nutrient uptake	upt^k_{PHY} k=NO_3, NH_4, PO_4, SiO; *PHY*=DA+NF+OP
Zooplankton dynamics:	
Grazing	$g_{l/q}$ l=MCZ, COP, NOC, AUR, MNE for l=MCZ q=BAC, NF l=COP q=DA, MCZ l=NOC q=DA, NF, OPP, BAC, MCZ, $PC_{1,2}$ l=AUR, MNE q=COP
Growth	μ_l l=MCZ, COP, NOC, AUR, MNE
Mortality	lys_l l=MCZ, COP, NOC, AUR, MNE
Egestion	eg_l l=MCZ, COP, NOC, AUR, MNE
Nutrient regeneration	reg^k_l l=MCZ, COP, NOC, AUR, MNE k=NH_4, PO_4
Microbial loop dynamics:	
C and nutrient uptake	upt^k_{BAC} k=BSC, BSN, NH_4, PO_4
Growth	μ_{BAC}
Mortality	lys_{BAC}
Ammonification	$reg^{NH_4}_{BAC}$
Nitrification	ni
Denitrification	dni
Ectoenzymatic hydrolyse of DOM	$elys_{Di}$ D_i=$DC_{1,2}$=$DN_{1,2}$=$DP_{1,2}$
Ectoenzymatic hydrolyse of POM	$elys_{Pi}$ P_i=$PC_{1,2}$=$PN_{1,2}$=$PP_{1,2}$
Sedimentation of POM	sed_{Pi} P_i=$PC_{1,2}$=$PN_{1,2}$=$PP_{1,2}$
Benthic dynamics:	
Nutrient exchanges at the sediment–water interface	$\mathcal{J}^k$ k=NO_3, NH_4, PO_4, SiO

TABLE A3. The BIOGEN model: conservation equations

Phytoplankton

Diatoms: $DA = DAF + DAS + DAR$

$$\frac{dDAF}{dt} = \mu_{DA} - lys_{DA} - \left[g_{NOC/DA} + g_{COP/DA}\right]\frac{DAF}{DA} - sed_{DAF}$$

$$\frac{dDAS}{dt} = \varphi_{DA} - e_{DAS} - s_{DAR} + c_{DAR} - \mu_{DA} - resp_{DA} - lys_{DAS} - \left[g_{NOC/DA} + g_{COP/DA}\right]\frac{DAS}{DA} - sed_{DAS}$$

$$\frac{dDAR}{dt} = s_{DAR} - c_{DAR} - lys_{DAR} - \left[g_{NOC/DA} + g_{COP/DA}\right]\frac{DAR}{DA} - sed_{DAR}$$

Autotrophic nanoflagellates: $NF = NFF + NFS + NFR$

$$\frac{dNFF}{dt} = \mu_{NF} - lys_{NFF} - \left[g_{MCZ/NF} + g_{NOC/NF}\right]\frac{NFF}{NF}$$

$$\frac{dNFS}{dt} = \varphi_{NF} - e_{NFS} - s_{NFR} + c_{NFR} - \mu_{NF} - resp_{NF} - \left[g_{MCZ/NF} + g_{NOC/NF}\right]\frac{NFS}{NF}$$

$$\frac{dNFR}{dt} = s_{NFR} - c_{NFR} - lys_{NFR} - \left[g_{MCZ/NF} + g_{NOC/NF}\right]\frac{NFR}{NF}$$

Opportunistic phytoplankton: $OP = OPF + OPS + OPR$

$$\frac{dOPF}{dt} = \mu_{OP} - lys_{OPF} - g_{NOC/OP}\frac{OPF}{OP} - sed_{OPF}$$

$$\frac{dOPS}{dt} = \varphi_{OP} - e_{OPS} - s_{OPR} + c_{OPR} - \mu_{OP} - resp_{OP} - lys_{OPS} - g_{NOC/OP}\frac{OPS}{OP} - sed_{OPS}$$

$$\frac{dOPR}{dt} = s_{OPR} - c_{OPR} - lys_{OPR} - g_{NOC/OP}\frac{OPR}{OP} - sed_{OPR}$$

Zooplankton

Microzooplankton: *MCZ*

$$\frac{dMCZ}{dt} = \mu_{MCZ} - lys_{MCZ} - g_{COP/MCZ} - g_{NOC/MCZ}$$

Copepods: COP

$$\frac{dCOP}{dt} = \mu_{COP} - lys_{COP} - eg_{COP} - g_{AUR/COP} - g_{MNE/COP}$$

Noctiluca: NOC

$$\frac{dNOC}{dt} = \mu_{NOC} - lys_{NOC} - eg_{NOC}$$

Aurelia: AUR

$$\frac{dAUR}{dt} = \mu_{AUR} - lys_{AUR} - eg_{AUR}$$

Mnemiopsis: MNE

$$\frac{dMNE}{dt} = \mu_{MNE} - lys_{MNE} - eg_{MNE}$$

Microbial loop

Bacteria: BAC

$$\frac{dBMC}{dt} = \mu_{BMC} - lys_{BMC} - g_{NOC/BMC} - g_{MCZ/BMC}$$

Organic matter: BSC, BSN, DC_i, DN_i, DP_I, PC_i, PN_i, PP_i (i=1,2)

$$\frac{dBSC}{dt} = elys_{DC1} + elys_{DC2} + lys_{DAS} + lys_{NFS} + lys_{OPS} + e_{DAS} + e_{NFS} + e_{OPS} - upt_{BAC}^{BSC}$$

$$\frac{dBSN}{dt} = elys_{DC1}\frac{DN1}{DC1} + elys_{DC2}\frac{DN2}{DC2} - upt_{BAC}^{BSN}$$

$$\frac{dDCi}{dt} = \varepsilon_{di} lys_{BIO} + \gamma_{di} eg_{ZOO} - elys_{DCi} + elys_{PCi}$$

$$\frac{dPCi}{dt} = \varepsilon_{p} lys_{BIO} + \gamma_{p} eg_{ZOO} - elys_{PCi} - sed_{PCi}$$

$$lys_{BIO} = lys_{DAF} + lys_{DAR} + lys_{NFF} + lys_{NFR} + lys_{OPF} + lys_{OPR} + lys_{BAC} + lys_{MCZ} + lys_{COP} + lys_{NOC} + lys_{AUR} + lys_{MNE}$$

$$eg_{ZOO} = eg_{COP} + eg_{NOC} + eg_{AUR} + eg_{MNE}$$

$$\frac{dDNi}{dt} = \varepsilon_d lysN_{BIO} + \gamma_d egN_{ZOO} - elys_{DCi}\frac{DNi}{DCi} + elys_{PNi}$$

$$\frac{dPNi}{dt} = \varepsilon_p lysN_{BIO} + \gamma_p egN_{ZOO} - elys_{PNi} - sed_{PNi}$$

$$lysN_{BIO} = \frac{lys_{DAF} + lys_{NFF} + lys_{OPF}}{CN_{PHY}} + \frac{lys_{BAC}}{CN_{BAC}} + \frac{lys_{MCZ} + lys_{COP} + lys_{NOC} + lys_{AUR} + lys_{MNE}}{CN_{ZOO}}$$

$$egN_{ZOO} = \frac{eg_{ZOO}}{CN_{ZOO}}$$

$$\frac{dDPi}{dt} = \varepsilon_d lysP_{BIO} + \gamma_d eg_{ZOO} - elys_{DCi}\frac{DPi}{DCi} + elys_{PNi}$$

$$lysP_{BIO} = \frac{lys_{DAF} + lys_{NFF} + lys_{OPF}}{CP_{PHY}} + \frac{lys_{BAC}}{CP_{BAC}} + \frac{lys_{MCZ} + lys_{COP} + lys_{NOC} + lys_{AUR} + lys_{MNE}}{CP_{ZOO}}$$

$$egP_{ZOO} = \frac{eg_{ZOO}}{CP_{ZOO}}$$

Nutrients

$$\frac{dNO_3}{dt} = -upt_{PHY}^{NO3} + ni - \frac{1}{z}\left[J^{NO3} + dni\right]$$

$$\frac{dNH_4}{dt} = -upt_{PHY}^{NH4} - ni - \frac{J^{NH4}}{z} + reg_{BAC}^{NH4} + reg_{MCZ}^{NH4} + reg_{COP}^{NH4} + reg_{NOC}^{NH4} + reg_{AUR}^{NH4} + reg_{MNE}^{NH4}$$

$$\frac{dPO_4}{dt} = -upt_{PHY}^{PO4} - upt_{BAC}^{PO4} - \frac{J^{PO4}}{z} + elys_{DCi}\frac{DPi}{DCi} + elys_{PC_2}\frac{PPi}{PCi} + reg_{MCZ}^{PO4} + reg_{COP}^{PO4} + reg_{NOC}^{PO4} + reg_{AUR}^{PO4} + reg_{MNE}^{PO4}$$

$$\frac{dSiO}{dt} = -upt_{DA}^{SiO} + k_b^{SiO} BSi$$

$$\frac{dBSi}{dt} = -k_b^{DSi} BSi + \frac{1}{CSi}\left[g_{NOC/DA} + g_{COP/DA} + sed_{DA}\right]\frac{DAF}{DA}$$

TABLE A4. The BIOGEN model: equations and parameters. Phytoplankton dynamics

Process		Equation	Parameters					
			Symbol	Description	DA	NF	OP	Unit
Photosynthesis	φ	$k_{max}(1-\exp-(aI/k_{max}))F$	$k^{\star}_{max}$	Maximal photosynthesis rate	0·355	0·355	0·355	h^{-1}
			a	Photosynthetic efficiency	0·0012	0·0012	0·0012	h^{-1} $(\mu Em^{-2}s^{-1})^{-1}$
Reserve synthesis	s_R	$\rho_{max}\frac{S/F}{k_s+S/F}F$	$\rho^{\star}_{max}$	Maximal rate of reserve synthesis	0·3	0·3	0·4	h^{-1}
			k_s	Half-saturation constant	0·06	0·06	0·06	dimensionless
Reserve catabolism	c_R	k_cR	$k^{\star}_c$	Rate of reserve catabolism	0·2	0·4	0·4	h^{-1}
Growth	μ	$\mu_{max}\frac{S/F}{k_s+S/F}\ln ut\ F$	$\mu^{\star}_{max}$	Maximal growth rate	0·155	0·165	0·155	h^{-1}
		with $\ln ut=\frac{(NO_3+NH_4)}{k_N+NO_3+NH_4}$	k_N	Half-saturation constant for inorganic nitrogen uptake	1	0·2	2·2	µM
		or $\frac{PO_4}{k_p+PO_4}$	k_P	Half-saturation constant for PO_4 uptake	0·1	0·02	0·2	µM
		or $\frac{SiO}{k_{Si}+SiO}$	k_{Si}	Half-saturation constant for Si uptake	1	—	—	µM
Respiration	$resp$	$k_mF+\zeta\mu$	k_m	Maintenance constant	0·0003	0·0005	0·0005	h^{-1}
			$\zeta^{\star\star\star}$	Biosynthesis cost	0·4–0·8	0·4–0·8	0·4–0·8	dimensionless
Exudation	e	$k_e\varphi$	k_e	Excretion constant	0·01	0·1	0·01	h^{-1}
Autolysis	lys_{PHY}	$k_{lys}(F+S+R)$	$k_{lys}^{\star\star}$	Autolysis constant	0·001	0·0025	0·002	h^{-1}
Sedimentation (DA, OP)	sed_{PHY}	$k_{sed}(F+S+R)$	$k_{sed}^{\star\star}$	Sedimentation rate constant	0·008	0	0·008	$m\ h^{-1}$
Inorganic N uptake	upt^N	µCN	CN	Phytoplankton stoichiometry C/N	4	4	4	µmol CF/µmol N
Ammonium preference (rpi)		$\left(\frac{NH_4}{NH_4+NO_3}\right)\alpha_{rpi}$	α_{rpi}	Relative preference index	0·3	0·4	0·75	dimensionless
PO_4 uptake	upt^P	µ/CP	CP	Phytoplankton stoichiometry C/P	80	80	80	µmol CF/µmol P
$Si(OH)_4$ uptake	upt^{Si}	µ/CSi	CSi	Phytoplankton stoichiometry $C/_{Si}$	2·8			µmol CF/µmol Si
Forcing temperature dependence: parameters with*								
p(T)		$p^{\star}\exp(-(T-Topt)^2/dti^2)$	Topt	Optimal temperature	22	22	24	°C
			dti	Temperature interval	12	12	12	°C
Limiting nutrient dependence: parameters with**								
p(lnut)		$p^{\star\star}(1+5)(1-lnut)$						
Inorganic nitrogen source—dependence: $\sigma^{\star\star\star}$								
ζ(N)		$0{\cdot}4rpi+0{\cdot}8(1-rpi)$						

PHY=F+S+R: PHY=DA, NF, OP.

TABLE A5. The BIOGEN model: equations and parameters. Zooplankton dynamics

Process		Equation	Parameters			
			Symbol	Description	Value	Unit
Microzooplankton: 2 preys: 1=BAC; 2=NF						
Grazing	g_{MCZ}	$gMCZ_{max}\Sigma[Prey_{1,2}/(kg_{app1,2}+Prey_{1,2})]$	$gMCZ_{max}$*	Maximal grazing rate	0·10	h^{-1}
		with: $kg_{app1}=kg_{BAC}(1+NF)/k_{gNF}$	kg_{BAC}	Half-saturation cst on BAC	15	mg C m^{-3}
		$kg_{app2}=kg_{NF}(1+BAC)/k_{gBAC}$	kg_{NF}	Half-saturation cst on NF	10	mg C m^{-3}
Growth	μ_{MCZ}	$Y_{MCZ}\ g_{MCZ}$	Y_{MCZ}	Growth efficiency	0·3	dimensionless
Autolysis	lys_{MCZ}	kd_{MCZ} MCZ	kd_{MCZ}	Mortality constant	0·003	h^{-1}
Copepods COP: 2 preys: 1=DA; 2=MCZ						
Grazing	g_{COP}	$gCOP_{max}\Sigma[Prey_{1,2}/(kg_{app1,2}+Prey_{1,2})]$	$gCOP_{max}$*	Maximal grazing rate	0·12	h^{-1}
		with: $kg_{app1}=kg_{DA}(1+MCZ)/k_{gMCZ}$	kg_{DA}	Half-saturation cst on DA	50	mg Cm^{-3}
		$kg_{app2}=kg_{MCZ}(1+DA)/k_{gDA}$	kg_{MCZ}	Half-saturation cst on MCZ	25	mg C m^{-3}
Growth	μ_{COP}	$Y_{COP}\ g_{COP}$	Y_{MZO}	Growth efficiency	0·33	dimensionless
Egestion	eg_{COP}	$E_Z\ g_{COP}$	E_Z	Egestion cst	0·25	dimensionless
Mortality	lys_{COP}	kd_{COP} COP	kd_{COP}*	Cst for total mortality	0·001	h^{-1}
Noctiluca						
Grazing	g_{NOC}	$\sum_i g_{iNOC}$	kg_{NOC}*	Ingestion coefficient	5×10^{-5}	h^{-1} mg C^{-1} m^{-3}
		with: $g_{iNOC}=kg_{NOC}(\sum_i Pi\text{-}TH_{NOC})P_i/\sum_i Pi$	TH_{NOC}	Feeding threshold	10	mg C^{-1} m^{-3}
		and i=DA, NF, OPP, BAC, MCZ, $PC_{1,2}$				
Growth	μ_{NOC}	$Y_{NOC}\ graz_{NOC}$	Y_{NOC}	Growth efficiency	0·15	dimensionless
Egestion	eg_{NOC}	Ez g_{NOC}	Ez	Egestion cst	0·25	dimensionless
Mortality	lys_{NOC}	kd_{NOC} NOC	kd_{NOC}*	Mortality cst	0·007	h^{-1}
Aurelia						
Grazing	g_{AUR}	$kg_{AUR}(COP-TH_{AUR})$	kg_{AUR}*	Ingestion coefficient	4×10^{-4}	h^{-1} mg C^{-1} m^{-3}
			TH_{AUR}	Feeding threshold	5	mg C^{-1} m^{-3}
Growth	μ_{AUR}	$Y_{AUR}\ g_{AUR}$	Y_{AUR}	Growth efficiency	0·15	dimensionless
Egestion	Eg_{AUR}	Ez g_{AUR}	Ez	Egestion cst	0·25	dimensionless
Mortality	lys_{AUR}	kd_{AUR} AUR	kd_{AUR}*	Mortality cst	4×10^{-4}	h^{-1}
Mnemiopsis						
Grazing	g_{MNE}	$kg_{MNE}(COP-TH_{MNE})$	kg_{MNE}*	Ingestion coefficient	6×10^{-4}	h^{-1} mg C^{-1} m^{-3}
			TH_{MNE}	Feeding threshold	10	mg C^{-1} m^{-3}
Growth	μ_{MNE}	$Y_{MNE}\ g_{MNE}$	Y_{MNE}	Growth efficiency	0·2	dimensionless
Egestion	eg_{MNE}	Ez g_{MNE}	Ez	Egestion cst	0·25	dimensionless
Mortality	lys_{MNE}	kd_{MNE} MNE	kd_{MNE}*	Mortality cst	6×10^{-4}	h^{-1}

TABLE A5. *Continued*

Parameter	Equation	Symbol	Signification	MCZ	COP	NOC	AUR	MNE
Temperature control: parameters with*								
p(T)	p*exp − (T − Topt)^2/ dti^2)	Topt	Optimal temperature	23 °C	23 °C	23 °C	23 °C	23 °C
		dti	Temperature interval	12 °C	8 °C	8 °C	12 °C	12 °C
Description	Value	Units						
Zooplankton stoichiometry								
C/N ratio	63	µg/µM						
N/P ratio	16	µM/µM						

TABLE A6. The BIOGEN model: equations and parameters. Microbial loop dynamics

Process		Equation	Parameters			
			Symbol	Signification	Value	Unit
$PC_{1,2}$ production by lysis and egestion		$\varepsilon_{p1,2}(lys_{PHY}+lys_{BAC}+lys_{MCZ}+lys_{COP}+lys_{NOC}+lys_{AUR}+lys_{MNE})$ $+\gamma_{p1,2}(eg_{COP}+eg_{NOC}+eg_{AUR}+eg_{MNE})$	ε_{p1}	PC_1 fraction in lysis products	0·1	dimensionless
			γ_{p1}	PC_1 fraction in egestion	0·3	
			ε_{p2}	PC_2 fraction in lysis products	0·4	dimensionless
			γ_{p2}	PC_2 fraction in egestion	0·4	
$PC_{1,2}$ ectoenzymatic hydrolysis	$elys_{P1,2}$	$k_{1,2}bPC_{1,2}$	$k_1b^\star$	PC_1 hydrolysis cst	0·005	h^{-1}
			k_2b	PC_2 hydrolysis cst	0·00025	h^{-1}
$PC_{1,2}$ sedimentation	$sed_{P1,2}$	(vsm/depth)	vsm	$PC_{1,2}$ sinking rate	0·01	$m\,h^{-1}$
$DC_{1,2}$ production by lysis and egestion		$\varepsilon_{d1,2}(lys_{PHY}+lys_{BAC}+lys_{MCZ}+lys_{COP}+lys_{NOC}+lys_{AUR}+lys_{MNE})$ $+\gamma_{d1,2}(eg_{COP}+eg_{NOC}+eg_{AUR}+eg_{MNE})$	ε_{d1}	DC_1 fraction in lysis products	0·3	dimensionless
			γ_{d1}	DC_1 fraction in egestion	0·1	dimensionless
			ε_{d2}	DC_2 fraction in lysis products	0·2	dimensionless
			γ_{d2}	DC_2 fraction in egestion	0·2	dimensionless
Ectoenzymatic hydrolysis of $DC_{1,2}$	$elys_{d1,2}$	$e_{1,2max}\dfrac{DC_{1,2}}{kh_{1,2}+DC_{1,2}}$	$e_{1max}^\star$	Maximum rate of DC_1 hydrolysis	0·75	h^{-1}
			$e_{2max}^\star$	Maximum rate of DC_2 hydrolysis	0·25	h^{-1}
			kh_1	Half saturation cst for DC_1 hydrolysis	250	$mg\,C\,m^{-3}$
			kh_2	Half saturation cst for DC_2 hydrolysis	2500	$mg\,C\,m^{-3}$
Monomers uptake BS=BSC, BSN	upt_{BAC}	$b_{max}\dfrac{BS}{k_{BS}+BS}$	$b_{max}^\star$	Maximum rate of BS uptake	0·4	h^{-1}
			k_{BS}	Half saturation cst for BS uptake	25	$mg\,C\,m^{-3}$
Bacterial growth	μ_{BAC}	$Y_{BAC}\,upt_{BAC}$	Y_{BAC}	Growth efficiency	0·2	dimensionless
PO_4 uptake	$upt_{BAC}^{PO_4}$	$\mu_{BAC}\dfrac{BAC}{CP_{BAC}}$	CP_{BAC}	Bacterial C/P ratio	106	$\mu M\,\mu M^{-1}$
Bacterial lysis	lys_{BAC}	$kd_{BAC}\,BAC$	$kd_{BAC}^\star$	Bacterial lysis rate cst	0·01	h^{-1}
Ammonification	$reg_{BAC}^{NH_4}$	$[(1-Y_{BAC})/Y_{BAC}]\mu_{BAC}/CN_{BAC}$	CN_{BAC}	Bacterial C/N ratio	4	$\mu M\,\mu M^{-1}$
Nitrification	ni	$ni_{max}\dfrac{NH_4}{k_{ni}+NH_4}$	ni_{max}	Maximum nitrification rate	0·03	$mM\,m^{-3}\,h$
			k_{ni}	Half-saturation cst	5	μM
Temperature forcing: parameters with p(T)		$p^\star\exp(-(T-Topt)^2/dti^2)$	Topt	Optimal temperature	30	°C
			dti	Temperature interval	18	°C

TABLE A7. The BIOGEN model: equations and parameters. Benthic diagenesis

Process	Equation	Parameters			
		Symbol	Signification	Value	Unit
Diffusion (interstitial phase)	Fick law	*Di*	Apparent diffusion coefficient	$1{\cdot}8 \times 10^{-5}$	$cm^2\ s^{-1}$
Mixing (solid phase)	Fick law	*Ds*	Mixing coefficient	$1{\cdot}8 \times 10^{-6}$	$cm^2\ s^{-1}$
Organic N mineralization	$k_{1,2}b\ PN_{1,2}$	$k_1b^\star$	PN_1 hydrolysis cst	0·005	h^{-1}
		k_2b	PN_2 hydrolysis cst	0·00025	h^{-1}
Organic P mineralization	$k_{1,2}p\ PP_{1,2}$	$k_{1p}^\star$	PP_1 hydrolysis cst	0·05	h^{-1}
		k_{2p}	PP_2 hydrolysis cst	0·0025	h^{-1}
Benthic nitrification (oxic layer)	$k_{nib1,2}\ NH_4$	$k_{nib1,2}$	First order nitrification cst	1	h^{-1}
NH_4 adsorption/desorption	1st order equilibrium	*Kam*	NH_4 adsorption cst	6	dimensionless
PO_4 adsorption/desorption (in benthos)	1st order equilibrium	*Kpa*	PO_4 adsorption cst (oxic)	35	dimensionless
		Kpe	PO_4 adsorption cst (anoxic)	1·7	dimensionless
BSi dissolution	$k_{BSi}BSi$	k_{BSi}	Silica dissolution cst	0·000075	h^{-1}
Temperature control: parameters with⋆					
p(T)	$p^\star\exp(-(T-Topt)^2/dti^2)$	Topt	Optimal temperature	30	°C
		dti	Temperature interval	18	°C